Neurobiology of Disease 83 (2015) 75–89

Contents lists available at ScienceDirect

Neurobiology of Disease

journal homepage: www.elsevier.com/locate/ynbdi

Genetic targeting of protease activated receptor 2 reduces inflammatory astrogliosis and improves recovery of function after spinal cord injury

Maja Radulovic [a,1], Hyesook Yoon [b,c,1], Jianmin Wu [b], Karim Mustafa [a], Michael G. Fehlings [d], Isobel A. Scarisbrick [a,b,c,*]

[a] Neurobiology of Disease Program, Mayo Medical and Graduate School, Rehabilitation Medicine Research Center, Rochester, MN 55905, United States
[b] Department of Physical Medicine and Rehabilitation, Mayo Medical and Graduate School, Rehabilitation Medicine Research Center, Rochester, MN 55905, United States
[c] Department of Physiology and Biomedical Engineering, Mayo Medical and Graduate School, Rehabilitation Medicine Research Center, Rochester, MN 55905, United States
[d] Department of Surgery, Toronto Western Research Institute, Toronto, ON M5T 2S8, Canada

ARTICLE INFO

Article history:
Received 7 April 2015
Revised 1 August 2015
Accepted 19 August 2015
Available online 24 August 2015

Keywords:
Traumatic spinal cord injury
Astrogliosis
Inflammation
Cytokine
GPCR
Serine protease

ABSTRACT

Inflammatory-astrogliosis exacerbates damage in the injured spinal cord and limits repair. Here we identify Protease Activated Receptor 2 (PAR2) as an essential regulator of these events with mice lacking the PAR2 gene showing greater improvements in motor coordination and strength after compression-spinal cord injury (SCI) compared to wild type littermates. Molecular profiling of the injury epicenter, and spinal segments above and below, demonstrated that mice lacking PAR2 had significantly attenuated elevations in key hallmarks of astrogliosis (glial fibrillary acidic protein (GFAP), vimentin and neurocan) and in expression of pro-inflammatory cytokines (interleukin-6 (IL-6), tumor necrosis factor (TNF) and interleukin-1 beta (IL-1β)). SCI in PAR2 −/− mice was also accompanied by improved preservation of protein kinase C gamma (PKCγ)-immunopositive corticospinal axons and reductions in GFAP-immunoreactivity, expression of the pro-apoptotic marker BCL2-interacting mediator of cell death (BIM), and in signal transducer and activator of transcription 3 (STAT3). The potential mechanistic link between PAR2, STAT3 and astrogliosis was further investigated in primary astrocytes to reveal that the SCI-related serine protease, neurosin (kallikrein 6) promotes IL-6 secretion in a PAR2 and STAT3-dependent manner. Data point to a signaling circuit in primary astrocytes in which neurosin signaling at PAR2 promotes IL-6 secretion and canonical STAT3 signaling. IL-6 promotes expression of GFAP, vimentin, additional IL-6 and robust increases in both neurosin and PAR2, thereby driving the PAR2-signaling circuit forward. Given the significant reductions in astrogliosis and inflammation as well as superior neuromotor recovery observed in PAR2 knockout mice after SCI, we suggest that this receptor and its agonists represent new drug targets to foster neuromotor recovery.

1. Introduction

Astrogliosis and inflammation are integrated contributors to the cascade of events occurring after spinal cord trauma. While certain components of this cascade worsen tissue damage and limit wound healing, other facets are essential to creating an environment favorable to repair. SCI-provoked astroglial and inflammatory responses fit on this complex continuum of injury and repair and this complicates targeted therapy. For example, the SCI-associated astroglial scar limits secondary damage by restricting inflammatory cell infiltration and providing mechanical support (Pekny et al., 1999; Okada et al., 2006; Herrmann et al., 2008; Wanner et al., 2013). In addition however, reactive astrocytes along with microglia and infiltrating macrophages secrete pro-inflammatory cytokines that can injure sparred axons and oligodendroglia (Klusman and Schwab, 1997; Kim et al., 2001; Okada et al., 2004; Wang et al., 2005). Moreover, the compact glial scar creates a chemical and physical barrier limiting regeneration of severed axons (Asher et al., 2001; Bradbury et al., 2002; Silver and Miller, 2004; Okada et al., 2006; Sofroniew, 2009). A better understanding of the molecular underpinnings of inflammatory-astrogliosis in SCI may enable selective targeting to foster an environment ultimately conducive to wound healing and compatible with emerging regenerative interventions.

Protease Activated Receptor 2 (PAR2) is a G-protein coupled receptor (GPCR) playing fundamental roles in neural injury, including effects across neurons, astrocytes and neuroinflammatory responses (Luo et al., 2007), although its activities in SCI are essentially unknown. There are four PARs (PARs1–4), each a classic seven transmembrane receptor. PARs are unique, being activated by cleavage within their extracellular domain to reveal a new amino-terminus that binds to the second extracellular loop to elicit intracellular signaling (Ramachandran et al., 2012).

* Corresponding author at: Neurobiology of Disease Program, 642B Guggenheim Building, Mayo Clinic Rochester, 200 First St., SW., Rochester, MN 55905, United States.
E-mail address: Scarisbrick.Isobel@mayo.edu (I.A. Scarisbrick).
[1] Designated co-first author, with authors contributing equally to the study.
Available online on ScienceDirect (www.sciencedirect.com).

http://dx.doi.org/10.1016/j.nbd.2015.08.021
0969-9961/

PARs enable cells to respond, or to over respond, to rapid changes in the proteolytic microenvironment occurring with CNS trauma, inflammation and blood brain barrier breakdown.

The role of PAR2 in neuropathogenesis is complex, depressing synaptic activity in hippocampal slices (Gan et al., 2011) and exacerbating neurotoxicity *in vitro* (Yoon et al., 2013) and in experimental autoimmune encephalomyelitis (Noorbakhsh et al., 2006). However, PAR2 serves a neuroprotective role in acute ischemic injury (Jin et al., 2005) and in human immunodeficiency virus-elicited neuroinflammation (Noorbakhsh et al., 2005). PAR2 activation also prevents ceramide-induced astrocyte apoptosis (Wang et al., 2007). The role of PAR2 in inflammation is also context specific, with anti-inflammatory actions in airways (Kouzaki et al., 2009) and intestine (Vergnolle et al., 2004), but pro-inflammatory effects in adjuvant induced arthritis (Ferrell et al., 2003), and allergic dermatitis (Kawagoe et al., 2002).

Given the unique position of PAR2 to mediate effects across multiple cell types in SCI, we sought to clarify its role and potential mechanism of action by determining the impact of PAR2 gene deletion on functional recovery and cellular and molecular signs of pathogenesis in murine experimental contusion–compression SCI. Complementary *in vivo* and *in vitro* approaches demonstrate that PAR2 can be targeted genetically to improve motor outcomes in SCI in part by limiting the canonical interleukin 6 (IL-6)-signal transducer and activator of transcription 3 (STAT3)-dependent signaling axis and the deleterious effects of inflammatory-astrogliosis.

2. Materials and methods

2.1. Experimental contusion–compression SCI

To investigate the role of PAR2 on neurobehavioral recovery after spinal cord trauma, we generated experimental SCI in twelve-week old (19–23 g) adult female PAR2 +/+ or PAR2 −/− (B6.Cg-F2rl1-^{tm1Nwb}) mice by application of a modified aneurysm clip (FEJOTA^{TM} mouse clip, 8 g closing force) as previously described (Joshi and Fehlings, 2002b; Yu and Fehlings, 2011; Radulovic et al., 2013). This model generates a severe injury with high clinical relevance related in part to the generation of an initial contusion as well as a persistent dorsal and ventral compression that results in a robust neuroinflammatory response, astrogliosis and axon degeneration (Joshi and Fehlings, 2002a, 2002b; Yu and Fehlings, 2011). PAR2 −/− mice were obtained from Jackson Laboratories (Bar Harbor, ME), backcrossed to C57BL/6 mice for more than 35 generations, and genotyped as described (Burda et al., 2013; Yoon et al., 2013). Uninjured PAR2 +/+ littermates served as controls in each case. The main endpoints examined were 3, 7 or 30 days after SCI (dpi), corresponding to acute and more chronic periods post-lesion.

Prior to spinal cord compression injury, mice were deeply anesthetized with Xylazine (0.125 mg/kg, Akom, Inc., Decatur, IL) and Ketaset (1 mg/kg, Fort Dodge Animal Health, Fort Dodge, IA). A laminectomy was performed and injury induced at the level of L1/L3 by extradural application of the FEJOTA clip for a period of 1 min. After surgery, the skin was repaired using AUTOCLIP (9 mm, BD Biosciences, San Jose, CA). Before and after surgery, 1 ml of saline was administered subcutaneously to replace lost blood volume. Pain was minimized by administration of Buprenorphine (0.05 mg/kg, Hospira, Lake Forest, IL) subcutaneously every 12 h for 96 h post-surgery. Food and water were available *ad libitum* and cage temperatures maintained at 37 C. To avoid infection, Baytril (10 mg/kg, Bayer Health Care, Shawnee Mission, KS) was administered intraperitoneally in a prophylactic fashion for the first 72 h post-surgery. Bladders were manually voided twice daily until the endpoint of each experiment. Any mice with signs of infection or which were moribund were immediately euthanized and excluded from the study. For all studies, mice were randomized with respect to genotype prior to surgery and investigators participating in surgery and evaluation of subsequent neurobehavioral or histological outcomes blinded to genotype throughout the duration of the experiment. Animals were housed in individual cages. All animal experiments were carried out with careful attention to animal comfort and in strict adherence to NIH Guidelines for animal care and safety. The Mayo Clinic Institutional Animal Care and Use Committee approved these studies.

2.2. Expression of PAR2 in experimental SCI

To address the potential significance of PAR2 to pathogenesis during the acute and more chronic periods after SCI, we determined the relative abundance of RNA expression for PAR2, and its CNS endogenous agonist, neurosin in RNA isolated from the uninjured spinal cord, or in the 3 mm of spinal cord at the level of the injury epicenter, as well as in the 3 mm above or below the site of injury site, at 7 or 30 dpi (n = 4 per time point). Neurosin is also commonly referred to as kallikrein 6 (Klk6) as well as Zyme, Protease M, or myelencephalon specific protease (MSP) (Scarisbrick and Blaber, 2012). Given the relatively low amount of RNA obtained from sites of injury, particularly at the injury epicenter and below at 30 dpi, samples from individual mice at a given endpoint and injury level were pooled prior to RNA isolation (Kendziorski et al., 2005; Radulovic et al., 2013). RNA was isolated using RNA STAT-60 (Tel-Test, Friendswood, TX) and stored at −70 C until the time of analysis. Amplification of the housekeeping gene 18S in the same RNA samples was used to control for loading. Real-time PCR amplification in each case was accomplished using primers obtained from Integrated DNA Technologies (Coralville, IA), or Applied Biosystems (Grand Island, NY), as detailed in Table 1, on an iCycler iQ5 system (BioRad, Hercules, CA).

2.3. Neurobehavioral outcome measures

All mice received training in the open field, ladder walk and incline plane test prior to surgery. A baseline measurement for each mouse in each assay was collected prior to surgery (0 dpi). The open field was used to assess seven categories of locomotor recovery using the Basso Mouse Scale (BMS), the day after surgery, and weekly thereafter until 30 dpi (Basso et al., 2006). Briefly, mice were placed in a plexiglass enclosed open field and 2 observers evaluated ankle movement, plantar placement, stepping, coordination, paw position, trunk stability and tail position generating a maximum BMS score of 9 and a subscore of 0 to 11.

The ladder walk was used to evaluate sensorimotor coordination between the hind limbs and forelimbs (Cummings et al., 2007). Mice were videotaped crossing a horizontal ladder fitted with an angled mirror to view/record footfalls prior to surgery and on days 8, 15, 22 and 31 after injury. 4 mm rungs of the ladder were spaced between 7.5 to 16 mm apart creating “easy” or “hard” levels of difficulty that included the

Table 1
Real time PCR assays used to quantify molecular changes in gene transcription in response to experimental contusion–compression SCI. Primers were obtained from Integrated DNA Technologies (IDT), or Applied Biosystems (AB), as indicated.

Gene	Accession number	Primer sequence forward/reverse
BIM	NM_207680	Probe Assay ID: Mm.PT.56a.8950841.g (IDT)
GFAP	NM_010277.2	GCAGATGAAGCCACCC TGG/GAGGTCTGGCTTGGCCAC (IDT)
IL-6	NM_031168.1	Probe Assay ID: Mm00446190_m1 (AB)
IL-10	NM_010548.2	Probe Assay ID: Mm00439614_m1 (AB)
IL-1β	NM_008361.3	Probe Assay ID: Mm.PT.51.17212823 (IDT)
Neurocan	NM_007789.3	Probe Assay ID: Mm.PT.56a.10993411 (AB)
Neurosin (Klk6)	NM_011177.2	CCTACCCTGGCAAGAT CAC/GGATCCATCTGATATGAGTGC
PAR2	NM_010170.4	GCATTGAACATCACCACCTG /GGATAGCCCTCTGCCTTTTC (IDT)
Rn18s	NR_003278.3	Probe Assay ID: Mm03928990_g1 (AB)
TGF-β1	NM_011577.1	Probe Assay ID: Mm01178820_m1 (IDT)
TNF	NM_013693.2	Probe Assay ID: Mm00443258_m1 (AB)
VIM	NM_011701.4	Probe Assay ID: Mm.PT.53a.8720419 (IDT)

possibility of 51 or 30 positive events (correctly placed steps), respectively. An independent observer evaluated the recorded steps without knowledge of genotype. In each case, the left and right hind limbs were scored for positive stepping events (plantar grasping, toe, skip), or foot-faults (miss, drag, spasm) and averaged to calculate the total number of positive events for each mouse.

The incline plane test was used to evaluate hind limb strength necessary to maintain a horizontal position on an inclined plane, with larger angles associated with better functional recovery. The last angle that each mouse could maintain stance for 5 s before turning was recorded and averaged across 3 attempts (Joshi and Fehlings, 2002a). Incline plane testing occurred after open field-testing weekly post-surgery starting on day 7.

2.4. Evaluation of histopathological recovery

At the 32 day endpoint, mice were deeply anesthetized with pentobarbital (100 mg/kg Nembutal, Abbott Laboratories, Chicago, IL) and perfused transcardially with 4% paraformalydehyde in phosphate buffered saline (pH 7.2) with spinal cords cut into 3 mm transverse segments. Five individual pieces encompassing the lesion epicenter, in addition to 2, 3 mm segments above and below, were embedded in a single paraffin block. 6 μm sections were stained with hematoxylin and eosin (H&E) to evaluate spinal cord gray or white matter area. In addition, immunoperoxidase methods were used to quantify the expression of the intermediate filament proteins, glial fibrillary acidic protein (GFAP, Z0334 Dako, Carpenteria, CA) or the presence of macrophages/microglia using an antibody recognizing Isolectin-B (Vector Laboratories, Inc. Burlingame, CA). An antibody recognizing the gamma subunit of protein kinase C (PKCγ sc-211 Santa Cruz, Dallas, TX) was used to evaluate the functional status of corticospinal axons (Mori et al., 1990; Bradbury et al., 2002; Lieu et al., 2013). Antigen staining in each case was carried out in parallel across genotypes using standard methods as we have previously described (Scarisbrick et al., 2002, 2006b; Blaber et al., 2004; Karimi-Abdolrezaee et al., 2010; Radulovic et al., 2013). Following incubation with primary antibodies, sections were washed in PBS and species appropriate AffiniPure F(ab′)2 fragment-specific biotin-conjugated secondary antibodies (Jackson ImmunoResearch, West Grove, PA) were applied for 1 h at RT. Antibody binding was visualized using HRP-conjugated streptavidin with 3′,3′-diaminobenzadine tetrahydrochloride (DAB) as the substrate. Processing of tissue sections with primary antibody replaced with normal serum was used to control for non-specific binding of secondary antibodies.

Measurements of spinal cord tissue area and the relative optical density (ROD) of the antigens stained were made using the KS-400 image analysis software (Carl Zeiss Vision, Hallbermoss, Germany) (Scarisbrick et al., 1999). Stained tissue sections encompassing the spinal injury epicenter and 2 segments above and below, were captured digitally at 5× (Olympus BX51 microscope and DP72 camera equipped with cellSens software 1.9 (Olympus, Center Valley, PA)), under constant illumination. Area measurements of the entire spinal cord section were made from H&E stained sections. ROD values determined for each antigen at a given segmental level were expressed as a percent of the total area measured. ROD values determined in each of the 2, 3 mm spinal segments examined above or below the injury epicenter were very similar and therefore mean measurements were combined for preparation of histograms and statistical analysis. A total of 9 spinal cords from PAR2 +/+ and 8 spinal cords from PAR2 −/− mice with SCI were stained and quantified. Four PAR2 +/+ and 4 PAR2 −/− uninjured controls were examined in parallel. Statistical differences between groups were compared using One Way ANOVA and the NK *post hoc* test, with $P < 0.05$ considered statistically significant.

Immunofluorescence techniques were used to determine the association of PAR2 or neurosin with astrocytes in the intact spinal cord and at 30 dpi. PAR2 was localized using a goat polyclonal antibody (sc-8205, Santa Cruz, Santa Cruz CA) and neurosin using a rabbit polyclonal antibody (Rb008) (Scarisbrick et al., 2012a; Radulovic et al., 2013). In each case, antibody binding was visualized using a species appropriate Alexa Fluor 488-conjugated secondary antibody (Jackson ImmunoResearch, West Grove, PA). GFAP was localized in the same tissue section using a CY3-conjugated GFAP antibody (C9206, Sigma, St. Louis, MO). All sections were counterstained with 4′,6-diamidino-2-phenylindole (DAPI) and imaged at 80× using an inverted laser scanning confocal microscope (LSM 780, Carl Zeiss Microscopy, LLC., Thornwood, NY).

2.5. Evaluation of molecular signatures of injury and repair

2.5.1. Protein expression

The impact of PAR2 gene deletion on SCI-induced astroglial scar formation as estimated by the expression of astroglial intermediate filament proteins, GFAP and vimentin, known to play key roles in formation of the glial scar (Wilhelmsson et al., 2004) were examined at the level of the injury epicenter, above and below at 3 and 30 dpi at a protein level using Western blot. In addition, given the well-established contribution of STAT3 to SCI-induced astrogliosis, its activation status was also examined in parallel to gain insight into the potential signaling pathways involved. To facilitate protein isolation, the 3 mm of spinal cord at a given segmental level (above, epicenter or below), from 3 to 4 mice at each of the 3 or 30 day time points, was homogenized collectively in radio-immunoprecipitation assay buffer. Protein samples (25 μg) from PAR2 +/+ or PAR2 −/− mice were resolved in parallel by electrophoresis on 10% to 12.5% SDS-PAGE gels (Bio-Rad Laboratories, Hercules, CA) and electroblotted onto nitrocellulose membranes. Multiple membranes were used to sequentially probe for antigens of interest, including GFAP (ab7260, Abcam, Cambridge, MA), vimentin (10366-1-AP, Proteintech, Chicago, IL), the phosphorylated or total protein forms of STAT3 (sc-8059, sc-8019, Santa Cruz, Santa Cruz, CA,) or BCL2-interacting mediator of cell death (BIM (2819S, Cell Signaling, Boston, MA)). All Western blots were re-probed with an antibody recognizing β-actin (NB600-501, Novus Biologicals, Littleton, CO) to control for loading. Signal for each protein of interest in samples derived from PAR2 +/+ or PAR2 −/− mice were detected on the same film using species appropriate horseradish peroxidase-conjugated secondary antibodies (GE Healthcare, Buckinghamshier, UK) and chemiluminescent techniques (Pierce, Rockford, IL). Films were scanned and the ROD of bands in each case was determined using Image Lab 2.0 software (Bio-Rad Laboratories). The ROD of each protein of interest was normalized to the ROD of actin detected on the same membrane and the mean and s.e. of these raw values across 3 to 4 separate Western blots used for analysis of the significance of the changes observed and for preparation of histograms.

2.5.2. RNA transcription

To determine the potential impact of PAR2 gene deletion on molecular signatures of SCI and repair at the level of gene transcription, we used real time PCR analysis of changes in cytokine, structural protein and apoptosis marker levels using real time PCR in spinal segments at the injury epicenter, above or below as described above. The specific probes and primers used to evaluate astrogliosis (GFAP, vimentin or neurocan), cytokines (TNF, IL-1β, IL-6, TGF-β1 or IL-10), and the pro-apoptotic marker BCL2-interacting mediator of cell death (BIM), are provided in Table 1 (Kendziorski et al., 2005; Radulovic et al., 2013). In the case of each gene of interest, samples from uninjured PAR2 +/+ or PAR2 −/− mice at a given time point, or segmental level, were amplified in parallel.

Statistical comparisons of changes in RNA transcription observed at the injury epicenter, as well as above and below, were made relative to that seen in the spinal cord of uninjured genotyped matched mice. In addition, potential differences in the baseline levels of each gene of interest in the uninjured spinal cord between PAR2 +/+ and PAR2 −/− mice were examined. To facilitate interpretation of the data, histograms are presented to show injury-induced transcriptional changes expressed as a percent of the uninjured control of the same

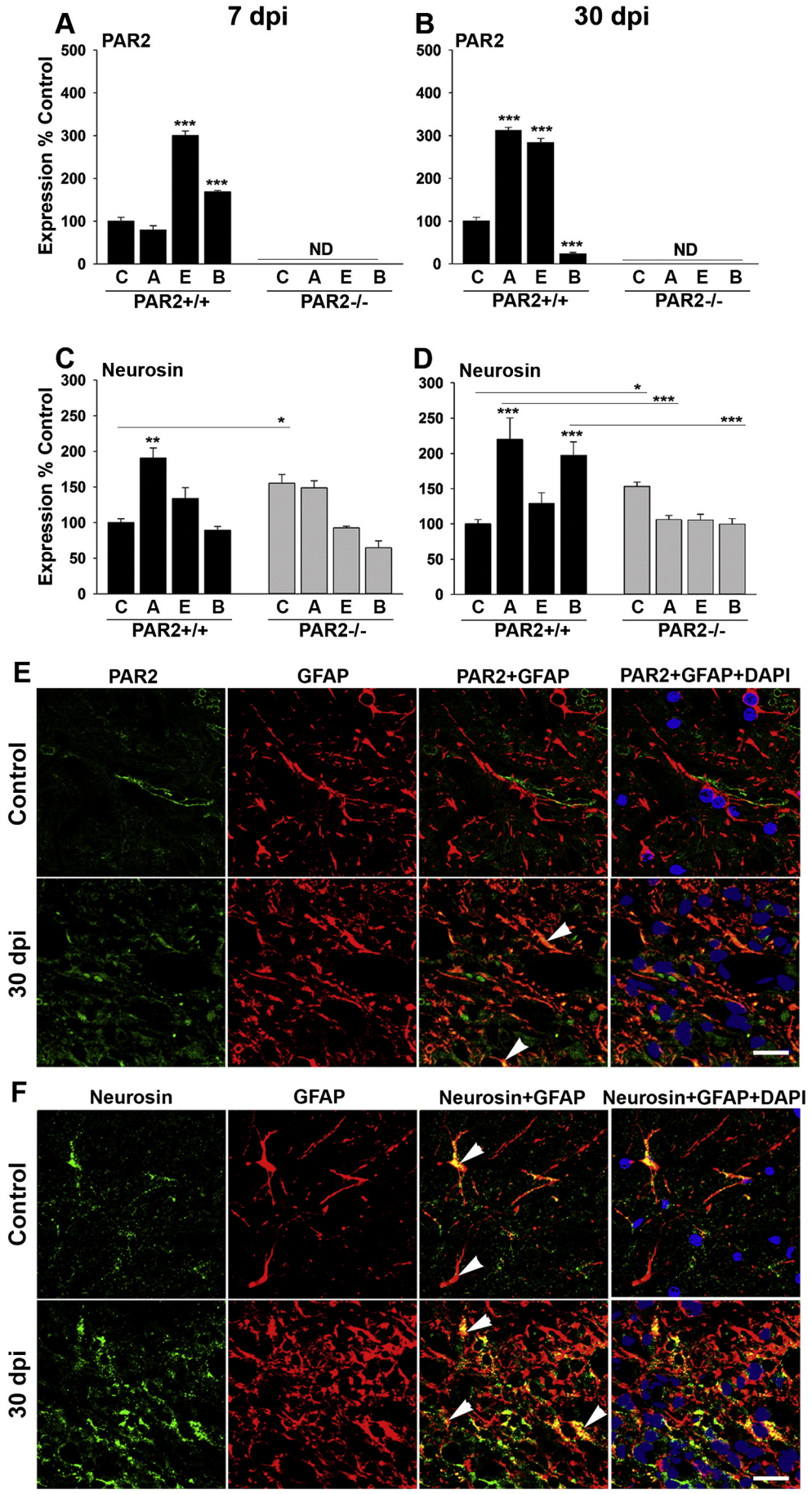
A
7 dpi
PAR2
Expression % Control
500
400
300
200
100
0
***
***
ND
C A E B
PAR2+/+
PAR2-/-
B
30 dpi
PAR2
***
***
***
ND
C A E B
PAR2+/+
PAR2-/-
C
Neurosin
Expression % Control
300
250
200
150
100
50
0
**
*
C A E B
PAR2+/+
PAR2-/-
D
Neurosin
*
***
***
***
***
C A E B
PAR2+/+
PAR2-/-
E
PAR2
GFAP
PAR2+GFAP
PAR2+GFAP+DAPI
Control
30 dpi
F
Neurosin
GFAP
Neurosin+GFAP
Neurosin+GFAP+DAPI
Control
30 dpi

genotype. However, to visualize any transcriptional-specific differences between PAR2 +/+ and PAR2 −/− uninjured mice, gene transcript levels in PAR2 −/− uninjured mice are presented as a percent of that observed in PAR2 +/+ uninjured spinal cords.

2.6. Astroglial cultures

Cultures of primary astrocytes derived from PAR2 +/+ or PAR2 −/− mice were used to critically evaluate the role of PAR2 in regulating the expression of key features of astrogliosis and the potential signal transduction pathway(s) involved. Primary astrocytes were purified from mixed glial cultures prepared from the cortices of postnatal day 1 mice as we have previously described (Scarisbrick et al., 2012a; Burda et al., 2013; Yoon et al., 2013). Mixed glial cultures were grown in media containing DMEM, 2 mM Glutamax, 1 mM sodium pyruvate, 20 mM HEPES, and 10% heat inactivated fetal calf serum (Atlanta Biologicals, Lawrenceville, GA). Purified astrocytes were obtained from 10 days *in vitro* mixed cultures by overnight shaking to remove oligodendrocyte progenitor cells and sequential panning on non-tissue culture treated plastic to eliminate microglia. The remaining bed of astrocytes was greater than 95% pure based on immunoreactivity for aldehyde dehydrogenase 1 family member L1 (ALDH1L1, ab87117, Abcam, Cambridge, MA, not shown). Astrocytes were trypsinized and plated across poly-L-lysine (Sigma, St. Louis, MO) coated 6 well plates in the same media at a density of 4.5×10^5 cells per well. Twenty-four hours later, media were replaced with defined Neurobasal A media containing 1% N2, 2% B27, 50 U/ml penicillin/streptomycin, 2 mM Glutamax, 1 mM sodium pyruvate, 0.45% glucose, and 50 μM β-mercaptoethanol (Sigma Aldrich, USA). All cells were maintained at 37 °C in 95% air and 5% CO_2, and all cell culture experiments were repeated independently at least 3 times.

Purified cultures of PAR2 +/+ astrocytes were used to determine the relative impact of the PAR2 agonist neurosin (Klk6, 150 nM), or the astrocyte-related pro-inflammatory cytokine IL-6 (20 ng/ml, National Cancer Institute, Frederick, MD), on the expression of GFAP, vimentin, or IL-6 RNA using quantitative real time PCR as described above (Table 1). Neurosin was expressed, purified and activated as we have previously described in detail (Scarisbrick et al., 2012a; Burda et al., 2013). To gain insight into a potential regulatory network between IL-6 and the PAR2 signaling axis, we also determined any impact on the expression of PAR2 and neurosin RNA. Astrocyte cultures were treated in triplicate for 24 h and RNA was isolated and amplified as described above. In addition, culture supernatants were collected and snap frozen to determine any impact on IL-6 secretion using Enzyme Linked Immunosorbant Assay (ELISA) according to the manufacturer instructions (eBioscience, San Diego, CA).

The role of PAR2 in regulating neurosin-mediated IL-6 secretion and the potential involvement of STAT3 were investigated in primary cultures of astrocytes derived from PAR2 +/+ or PAR2 −/− mice. In addition, we evaluated whether neurosin-elicited IL-6 secretion was blocked by a small molecule inhibitor of STAT3 (Stattic, 5 or 20 μM, Tocris Bioscience, Minneapolis, MN) or mitogen-activated protein kinase (MAPK)/ERK (MEK1/2) (U0126, 150 μM, Tocris Bioscience). Cultures were pretreated with inhibitors for 1 h prior to application of neurosin and supernatants collected 24 h later for examination of IL-6 secretion. Alternatively, cultures were harvested into radio-immunoprecipitation assay buffer for quantification of STAT3 activation by Western blot as described above.

2.7. Statistical analysis

Statistical significance in the case of histological and molecular outcomes across multiple groups was evaluated using One Way Analysis of Variance (ANOVA) with the NK *post-hoc* test or non-parametric ANOVA on RANKS with Dunn's test. Statistical differences between two groups were determined with Students t-test or Mann–Whitney U for non-parametric data. To evaluate the impact of genotype on functional outcomes over time after injury, BMS scores and subscores, ladder walk and incline plane assessments were analyzed using a Two-Way Repeated Measures ANOVA with fixed effects and the Newman Keuls (NK) *post-hoc*. All data are presented as mean ± standard error of the mean (s.e.). In all cases, $P < 0.05$ was considered statistically significant.

3. Results

3.1. Experimental murine SCI induces transcriptional elevations in RNA encoding PAR2 and its agonist, neurosin, in wild type but not PAR2 gene deficit mice

To determine the contribution of PAR2 to the pathogenesis of traumatic SCI, we quantified changes in PAR2 RNA at the injury epicenter and in segments above and below at 7 and 30 dpi (Fig. 1, A–B). At the level of injury, PAR2 RNA was increased by 2.8 to 3-fold at 7 dpi and 30 dpi ($P < 0.001$, NK). PAR2 was also significantly elevated above the epicenter (3.1-fold) at 30 dpi ($P < 0.001$, NK). Below the epicenter, PAR2 RNA was increased by 1.8-fold at 7 dpi, but reduced nearly 5-fold by 30 dpi ($P \leq 0.002$, NK).

The level of the PAR2 agonist neurosin (Klk6) was also determined at 7 and 30 dpi (Fig. 1, C–D). In PAR2 +/+ mice, neurosin RNA levels were elevated 1.7-fold above the epicenter at 7 dpi and 2-fold above the epicenter and below by 30 dpi ($P \leq 0.01$, NK). In mice lacking the PAR2 gene, neurosin RNA levels at baseline were 1.5-fold higher relative to uninjured PAR2 +/+ mice ($P = 0.03$, NK). Contrasting the increases seen in neurosin RNA expression after SCI in PAR2 +/+ mice, mice lacking the PAR2 gene showed no significant changes in neurosin at 7 or 30 dpi.

To assess whether PAR2 is directly associated with astrocytes, we examined co-localization of PAR2 and GFAP in the uninjured spinal cord and within the SCI epicenter at 30 dpi using immunofluorescence (IF) techniques (Fig. 1E). In the intact adult spinal cord, levels of PAR2-IF were overall low appearing most dense in association with the luminal surface of blood vessels rather than astrocytes. Neurosin was expressed by a subset of GFAP-IF astrocytes in the intact spinal cord (Fig. 1F) as previously described (Scarisbrick et al., 2006b). The number of astrocytes immunoreactive for both GFAP and PAR2, or for GFAP and neurosin, was increased at 30 dpi.

3.2. PAR2 gene deletion is associated with improved motor recovery after SCI

Before injury, wild type and PAR2 −/− mice displayed identical patterns of motor activity in the open field test, on ladder walk, and in the incline plane test (Fig. 2, A–E). The day following contusion–compression

Fig. 1. The expression of PAR2 and neurosin (Klk6) are elevated in response to contusion–compression SCI. Histograms show transcriptional changes in RNA encoding PAR2 in the spinal cord of uninjured control (C) PAR2 +/+ mice, or at the level of the injury epicenter (E), above (A), or below (B), at 7 and 30 dpi (A, B). PAR2 RNA was not detected (ND) in PAR2 −/− mice. In PAR2 +/+ mice, co-ordinate elevations were seen in the SCI-related secreted serine protease neurosin, already established to activate nervous system PAR2 (Vandell et al., 2008; Yoon et al., 2013). By contrast, in mice lacking the PAR2 gene, significant elevations in neurosin in response to SCI were not observed (C, D). (*$P < 0.03$; **$P = 0.009$, ***$P \leq 0.001$ NK; ND, not detected). Photomicrographs show co-localization of PAR2 and GFAP (E), or neurosin and GFAP (F), in the uninjured spinal cord (Control) and within the injury epicenter at 30 dpi. Increases in GFAP-positive cells co-labeled for PAR2 or neurosin were observed at 30 dpi and a selection of double labeled cells in each case is shown at arrowheads (Scale bar = 20 um).

injury, both groups were equally impaired in the open field test with a mean BMS score of 1.2 ± 0.1 in PAR2 +/+ and 1.4 ± 0.1 in PAR2 −/− mice. Across both groups mice began to show significant improvements in BMS scores by 7 dpi, with progressive increases thereafter. Recovery in BMS scores in PAR2 −/− mice was significantly higher than PAR2 +/+ mice at 7 dpi through 30 dpi ($P \leq 0.04$, NK). At the 30 day endpoint, BMS scores in PAR2 −/− were an average of 2.1 points higher than their wild type littermates. Improvements in BMS subscores were first observed in both groups by 14 dpi, with those in PAR2 −/− significantly higher than those in PAR2 +/+ mice from 14 dpi onward ($P < 0.001$, NK). At the 30 day endpoint, BMS subscores in PAR2 −/− were an average of 3.4 points higher than their wild type littermates.

Significant improvements in the easy ladder walk test were observed by 15 dpi, with PAR2 −/− mice showing significantly higher levels of recovery at this time point, as well as at 22, and 31 dpi ($P \leq 0.02$, NK). Significant improvements in the hard ladder walk test were observed by 8 dpi with PAR2 −/− mice achieving a higher number of positive events ($P = 0.006$, NK). Enhanced recovery on the hard ladder walk test continued when evaluated on days 15, 22 and 31 ($P < 0.05$, NK). Significant improvements in the Incline plane test (over those observed at 7 dpi) were observed in both PAR2 +/+ and PAR2 −/− mice by 14 dpi, with significantly higher mean maximal angles achieved by PAR2 −/− over wild type mice at 30 dpi ($P \leq 0.04$, NK).

3.3. PAR2 gene deletion is associated with improvements in neuropathological outcomes

Spinal cord areas in intact mice and after SCI were quantified in H&E stained sections at the level of the injury epicenter, above and below at the 32 day endpoint of each experiment (Fig. 3). As expected, compression injury resulted in 2 to 3-fold reductions in spinal cord area at the level of the injury epicenter and below ($P < 0.001$, NK). In this model, there were no significant changes in spinal cord areas above the injury epicenter at 32 dpi. There was a 62% decrease in mean spinal cord area at the level of the lesion epicenter 32 dpi in PAR2 +/+ relative to intact mice. Loss of spinal cord tissue at the level of the injury epicenter was reduced in mice lacking the PAR2 gene (44% decrease in mean area) a significant improvement in tissue sparring relative to their wild type littermates ($P = 0.04$). There were no differences is spinal cord tissue loss below the injury epicenter between PAR2 +/+ and PAR2 −/− mice.

To determine whether the absence of PAR2 impacted inflammatory astrogliosis at a neuropathological level, we quantified immunoreactivity (IR) for GFAP and for Isolectin B as a marker of activated microglia and infiltrating monocytes at the 32 day endpoint of each experiment (Fig. 3 J to U). As expected, GFAP-IR in wild type mice was increased 2 to 3-fold in response to compression SCI in the injury epicenter, above and below ($P < 0.001$, NK). Elevations were also observed in GFAP-IR in PAR2 −/− mice in the injury epicenter, but these did not reach the level of statistical significance and were significantly lower than those observed in wild type mice ($P < 0.001$). In both wild type and PAR2 −/− mice at 32 dpi, immunoreactivity for Isolectin B remained significantly elevated in the injury epicenter (up to 28-fold). Elevations in Isolectin B also persisted below the level of injury in wild type mice (9-fold) relative to that in the uninjured spinal cord, but not in PAR2 −/− mice ($P = 0.004$). Finally, we examined PKCγ-IR within the corticospinal tract as a marker of the functional status of this descending motor pathway (Fig. 3 V to Z) (Mori et al., 1990; Bradbury et al., 2002; Karimi-Abdolrezaee et al., 2010; Lieu et al., 2013). PKCγ-IR was significantly reduced in spinal segments above and below the lesion epicenter in PAR2 +/+ mice ($P < 0.001$, NK). Smaller injury-associated-reductions in PKCγ were observed in PAR2 −/− relative to PAR2 +/+ mice above the level of injury ($P \leq 0.04$, NK). Within the lesion epicenter, axons immunoreactive for PKCγ were below the detection limit of our assay at 32 dpi in both wild type and PAR2 −/− mice.

3.4. PAR2 gene deletion reduces key hallmarks of SCI-driven astrogliosis in vivo

Quantitative Western blot approaches were used to further evaluate the impact of PAR2 gene deletion on molecular hallmarks of astrogliosis, including GFAP and vimentin (Lepekhin et al., 2001; Pekny and Pekna, 2004; Wilhelmsson et al., 2004) after SCI at 3 and 30 dpi and the potential signaling pathways involved (Fig. 4). As expected, substantial elevations in GFAP protein were observed after SCI with the most prominent elevations occurring at the injury epicenter and below at acute stages (3 dpi), and at the injury epicenter and above at the chronic 30 dpi end point ($P \leq 0.01$, NK). The observed elevations in GFAP protein in the injury epicenter and below at 3 dpi in PAR2 +/+ mice were completely absent in mice lacking PAR2 ($P \leq 0.001$, NK). Protein levels of vimentin, another intermediate filament protein involved in astrogliosis, were below the detection limit of the Western in the uninjured spinal cord and at 3 dpi (Fig. 4). Vimentin is highly expressed in the developing nervous system, down regulated postnatally and re-expressed after SCI (Wilhelmsson et al., 2004). Elevations in vimentin protein were evident 30 dpi when significant increases were observed at the level of the injury epicenter (75-fold) and below (35-fold) in PAR2 +/+ mice ($P \leq 0.01$, NK). Elevations in vimentin protein observed at 30 dpi in wild type mice were absent at all levels of SCI examined in PAR2 −/− mice.

Signal transducer and activator of transcription 3 (STAT3) is a signal transduction pathway known to participate in the response of the CNS to injury, including inflammation (Kim et al., 2002; Dominguez et al., 2010) and astrogliosis (Okada et al., 2006; Herrmann et al., 2008). Given the impact of PAR2 −/− in reducing both inflammation and astrogliosis after SCI we evaluated whether STAT3 signaling may also be impacted. As expected, levels of activated STAT3 were elevated in PAR2 +/+ mice at 3 and 30 dpi ($P \leq 0.01$, NK, Fig. 4). Elevated levels of activated STAT3 observed below the epicenter at 3 dpi, and at the injury epicenter 30 dpi, were reduced in mice lacking PAR2 ($P \leq 0.001$ NK). In addition, elevations in total STAT3 seen at the injury epicenter and below at 30 dpi were completely blocked in mice PAR2 lacking the PAR2 gene ($P < 0.05$, NK).

3.5. PAR2 regulates molecular signatures of inflammatory-astrogliosis and apoptosis in experimental traumatic SCI

3.5.1. Astroglial-associated RNA transcription

The impact of PAR2 gene deletion on SCI-induced astrogliosis was further evaluated by determining changes in gene transcription for GFAP, vimentin and neurocan (Fig. 5 A–C). Among the key indices examined, the intermediate filament protein vimentin was transcriptionally most dynamic reaching levels more than 30-fold higher than uninjured controls in the injury epicenter 30 dpi ($P \leq 0.001$ NK). Parallel, albeit lower elevations in vimentin transcription were seen at the same time points above and below the level of injury, where increases were 5- to 10-fold that in the intact spinal cord. Mice lacking PAR2 showed reduced elevations in vimentin RNA expression relative to PAR2 +/+ mice ($P \leq 0.001$, NK).

As expected, GFAP RNA was elevated in response to spinal cord contusion–compression injury, with significant increases across the levels of injury examined reaching 2- to 3-fold that in the intact spinal cord 30 dpi ($P \leq 0.001$ NK, Fig. 5A). Elevations in GFAP were also observed at 30 dpi in PAR2 −/− mice at each level except in segments above the injury epicenter.

Moderate (1.3-fold) elevations in neurocan RNA were observed above the SCI epicenter in PAR2 +/+ mice at 30 dpi ($P = 0.04$, NK) and these increases were attenuated in mice lacking PAR2 ($P = 0.02$, NK, Fig. 5C). While neurocan was elevated in spinal segments above the site of injury in PAR2 +/+ mice, it was expressed at lower than baseline levels in the injury epicenter and below in PAR2 +/+ and

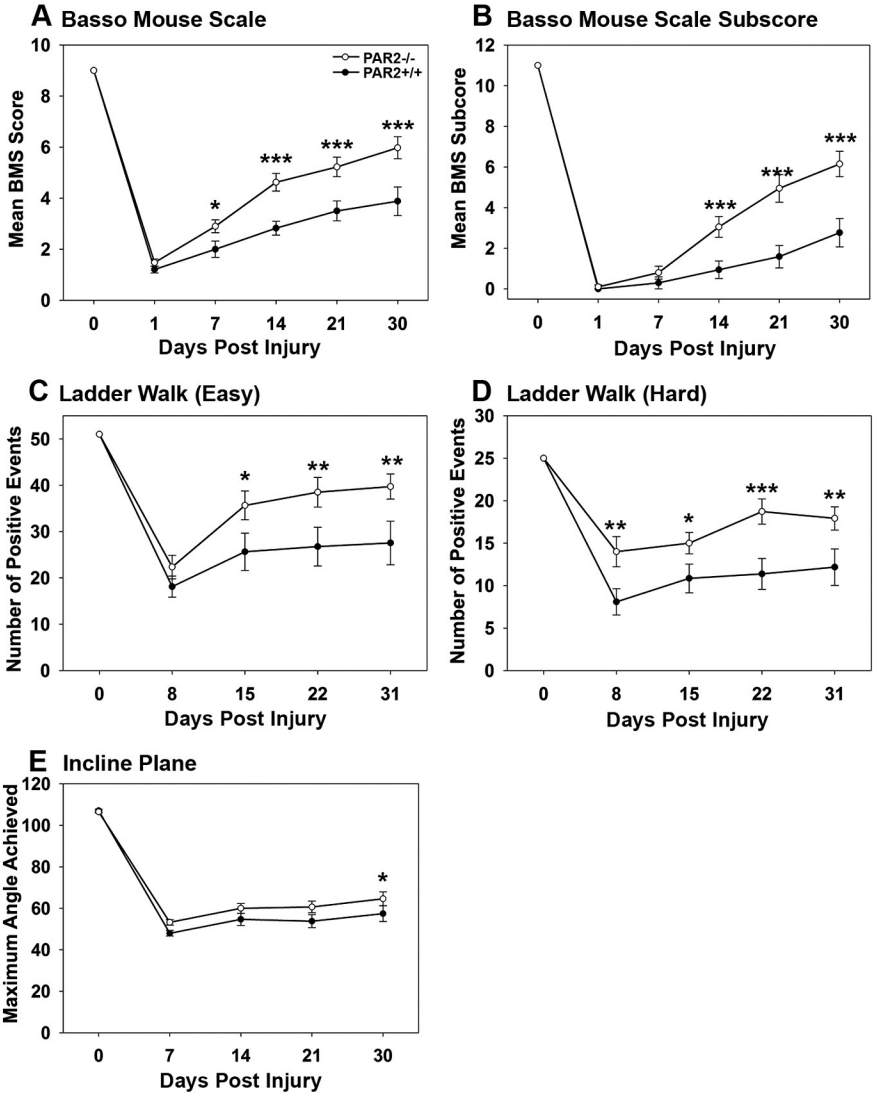

Fig. 2. PAR2 gene deficient mice show improved locomotor recovery after experimental contusion–compression SCI. (A) Basso Mouse Scale (BMS) scores evaluated in PAR2 +/+ and PAR2 −/− mice from 0 to 31 days after SCI, demonstrate significant improvements in over-ground locomotion. Significantly higher levels of recovery on the BMS were observed in PAR2 −/− mice at 7 dpi ($P = 0.045$) and at each time point thereafter ($P < 0.001$). (B) BMS subscores were significantly higher in PAR2 −/− compared to PAR2 +/+ mice starting on 14 dpi and continuing through the last time point examined ($P < 0.001$). (C, D) Improvements in stepping accuracy in the easy and hard rung spacing ladder walk tests were observed by 15 dpi and persisted when examined at 22 and 31 dpi. Improvements in ladder walk accuracy were also observed at 8 dpi in PAR2 −/− relative to PAR2 +/+ mice in the hard set up. (E) PAR2 −/− mice showed significantly better motor strength in the incline plane test at 30 dpi relative to that observed in PAR2 +/+ mice. Data shown represents the mean and standard error of results obtained across two independent experiments, PAR2 +/+, n = 17; PAR2 −/− n = 20. (Two Way Repeated Measures ANOVA, NK *$P < 0.05$, **$P \le .008$, ***$P < 0.001$).

PAR2 −/− mice. Neurocan expression levels in the intact spinal cord were higher in PAR2 −/− compared to PAR2 +/+ mice ($P < 0.01$, NK).

3.5.2. Apoptosis-associated RNA transcription and Protein Expression

Substantial elevations in the pro-apoptotic signaling protein BIM were observed in response to contusion–compression spinal cord injury with levels reaching 3 to 8-fold that observed in the intact spinal cord 30 dpi ($P \le 0.001$ NK, Fig. 5F). Mice lacking the PAR2 gene showed substantially lower levels of BIM induction above the SCI at the injury epicenter and above ($P \le 0.002$, NK) 30 dpi. BIM protein levels were also highly elevated at 30 dpi in the injury epicenter and below and these changes were significantly reduced in mice lacking PAR2 ($P \le 0.02$, NK, Fig. 5D and E).

3.5.3. Cytokine RNA transcription

Pro- and anti-inflammatory cytokines are altered at sites of CNS injury due to changes in expression by astrocytes and microglia, as well as infiltrating immune cells and neurons in some cases (Bastien and Lacroix, 2014) and their possible contribution to improved neurobehavioral recovery after SCI in PAR2 −/− mice was examined using quantitative real time PCR (Fig. 6). Across the cytokines examined, which included 3 different pro-inflammatory cytokines (TNF, IL1-β and IL-6), and 2 generally anti-inflammatory cytokines (TGF-β and IL-10), the greatest increases in RNA transcription observed occurred at the level of the injury epicenter with smaller elevations above and below. The magnitude of changes in cytokine expression in PAR2 −/− mice was overall reduced relative to that observed in PAR2 +/+ mice. In the uninjured spinal cord, no significant differences in cytokine expression were observed as a result of PAR2 gene deletion.

The most dynamic changes in cytokine RNA expression relative to the uninjured spinal cord were observed for IL1-β which was 59-fold higher in the SCI epicenter of PAR2 +/+ mice relative to uninjured cord at 30 dpi, respectively ($P < 0.001$, NK, Fig. 6B). Transcriptional elevations in IL1-β were attenuated in PAR2 −/− mice with 3-fold lower elevations in the injury epicenter ($P < 0.001$, NK). Elevations in IL1-β above the injury site were also reduced in PAR2 −/− mice ($P < 0.001$, NK).

The expression of TNF RNA at the SCI epicenter in PAR2 +/+ mice was highly elevated at 30 dpi (28-fold) ($P < 0.001$, NK, Fig. 6A).

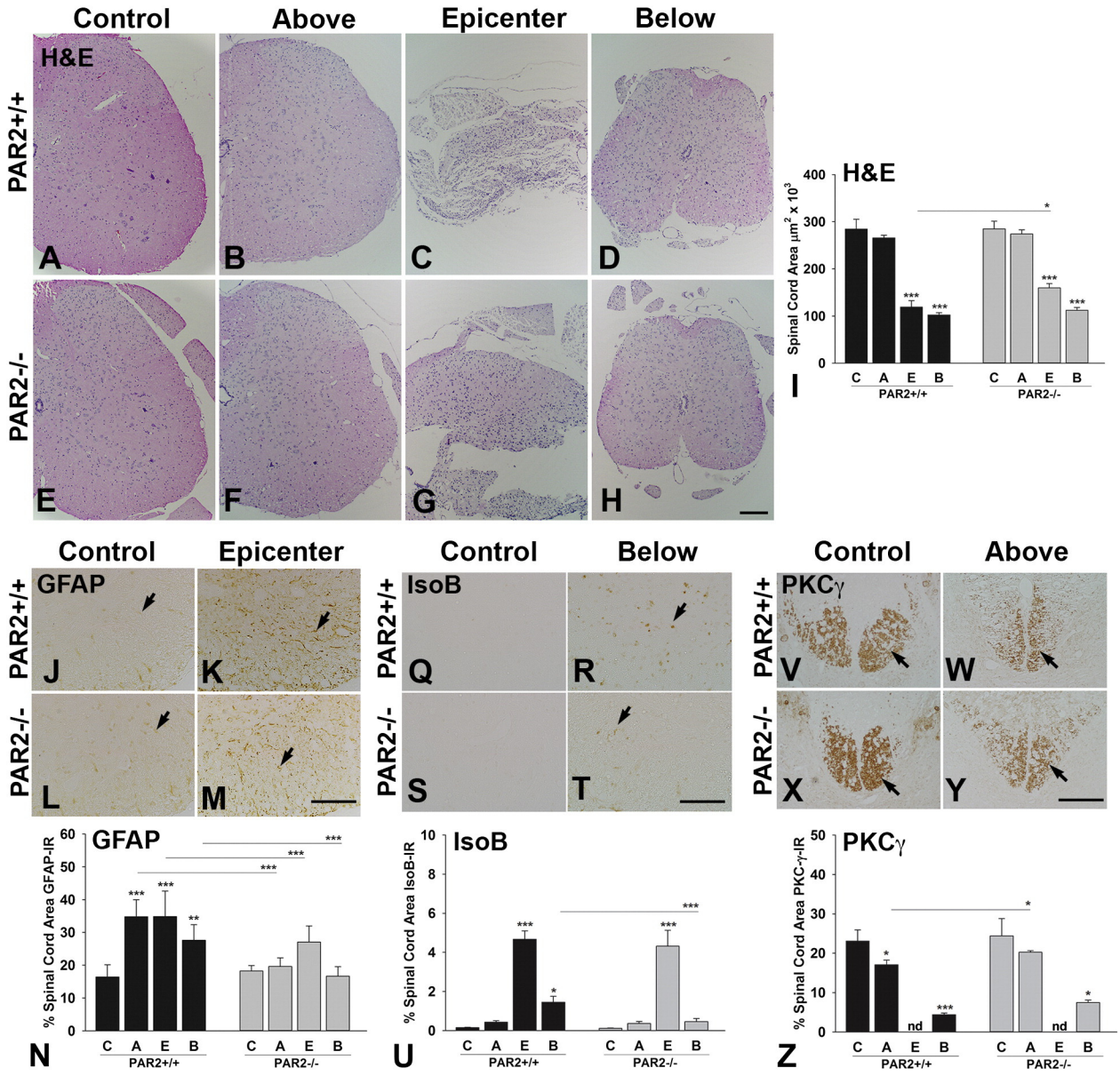

Fig. 3. PAR2 gene deletion is associated with reduced inflammatory astrogliosis, tissue sparring and greater preservation of PKCγ-immunopositive corticospinal tract axons after experimental contusion–compression SCI. Photomicrographs and associated histograms show measurements of spinal cord areas taken from H&E stained sections (A to I), or the percent of spinal cord area immunoreactive for GFAP (J to N), or Isolectin B-IR (IsoB) microglia/macrophages (Q to U), at the 32 day endpoint of each experiment. In addition, the % area at the base of the dorsal column white matter stained for PKCγ, as a measure of corticospinal axon function (V to Z), was evaluated. In each case, measurements were made in spinal cord sections taken from the level of the injury epicenter (E), above (A), or below (B). Arrows J to Y indicate an example of significant immunostaining in each case. In mice lacking PAR2 there was tissue sparring at the level of the injury epicenter (I), reductions in GFAP-IR at the injury epicenter, above and below (N), reductions in IsoB-IR below and preservation of PKCγ-IR in spinal segments above the site of lesion (PAR2+/+, n = 13 (4 Control, 9 SCI); PAR2 −/−, n = 12 (4 Control, 8 SCI); *P < 0.05, **P ≤ 0.01, ***P ≤ 0.001 NK). Scale Bar A–H = 250 μm; J–Y = 100 μm.

Elevations in TNF were completely absent in PAR2 −/− mice at all levels of SCI examined at 30 dpi (P < 0.001, NK).

IL-6 RNA expression was up regulated in the SCI epicenter of PAR2 +/+ mice by 4-fold at 30 dpi (P < 0.001, NK, Fig. 6C). In PAR2 −/− mice, elevations in IL-6 were reduced above and at the SCI epicenter at 30 dpi (P < 0.001, NK).

TGF-β RNA expression was elevated after SCI at all injury levels 30 dpi with the highest levels of expression occurring in the epicenter with 14-fold elevations in PAR2 +/+ and 9.5-fold elevations in PAR2 −/− mice (P < 0.001, NK, Fig. 6D). TGF-β expression was also reduced above the epicenter in PAR2 −/− relative to PAR2 +/+ mice at 30 dpi (P = 0.003, NK).

IL-10 expression was elevated in the injury epicenter as well as above and below in PAR2 +/+ mice by 4 to 6-fold at 30 dpi (P < 0.001, NK, Fig. 6E). In PAR2 −/− mice, elevations in IL-10 RNA below the epicenter at 30 dpi (10-fold) were significantly reduced relative to wild type mice (P < 0.002, NK).

3.6. IL-6 drives expression of the PAR2-signaling axis and markers of astrogliosis in primary astrocytes in vitro

Given the significant impact of PAR2-loss-of function on SCI-induced astrogliosis and pro-inflammatory cytokine production, we sought to determine if these effects are linked at the level of the astrocyte (Fig. 7). Treatment of primary astrocytes with the PAR2 agonist neurosin for 24 h promoted a 1.5-fold increase in IL-6 secretion (P = 0.004, Student t-test). In turn, recombinant IL-6 promoted a 2 to 3-fold increase in the expression of GFAP or vimentin RNA (P ≤ 0.001, Student t-test). Notably recombinant neurosin was not found to be a significant driver of the expression of these astroglial intermediate

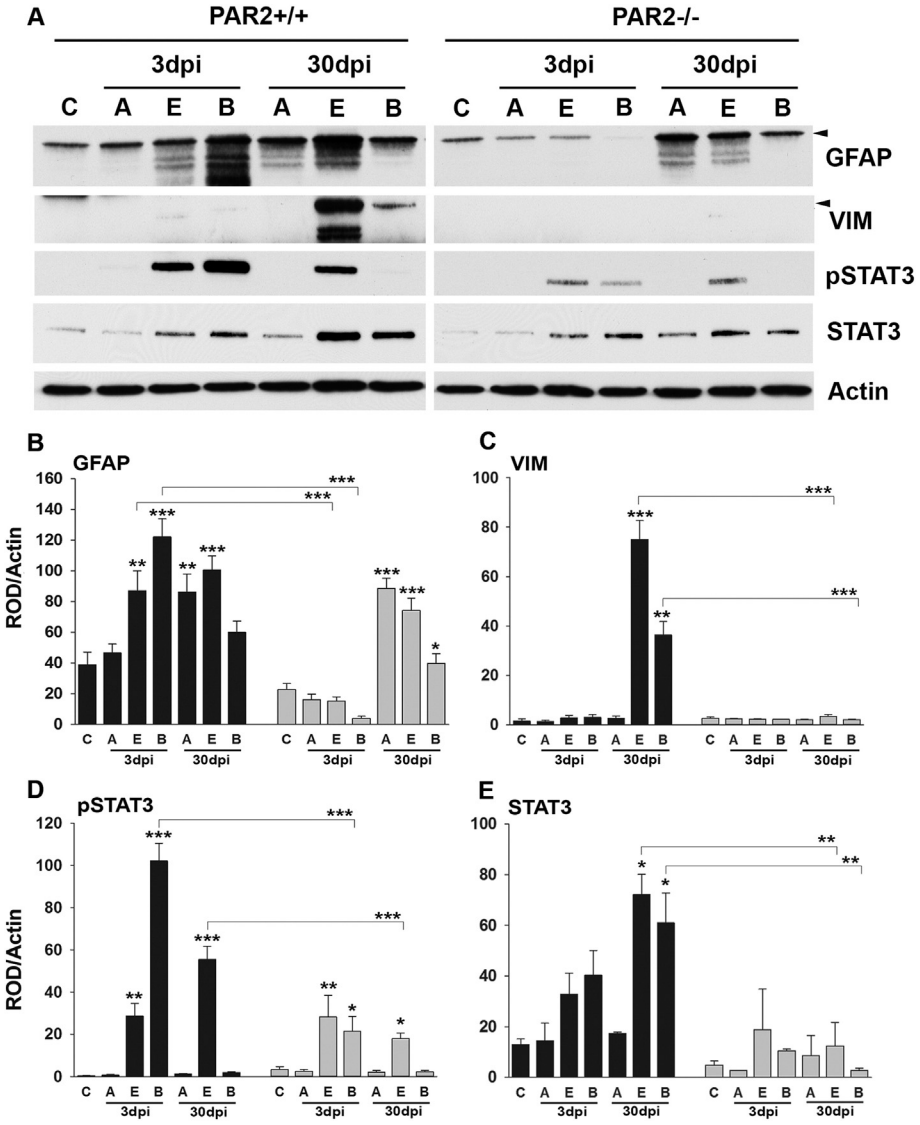

Fig. 4. Spinal cord injury-associated elevations in GFAP, vimentin and STAT3 signaling were reduced in PAR2 gene deficient mice. Western blots and corresponding histograms show differential expression of GFAP, vimentin (VIM), pSTAT3 and STAT3 in the uninjured (C, Control) or injured PAR2 +/+ or PAR2 −/− spinal cord at 3 or 30 dpi. Protein samples isolated from the injury epicenter (E), above (A), or below (B) from PAR2 +/+ or PAR2 −/− mice were examined in parallel with uninjured samples in each case and results developed on the same film. SCI-induced elevations in GFAP, vimentin and STAT3 were all significantly reduced in mice lacking the PAR2 gene. In some cases, multiple bands for GFAP or vimentin were detected after SCI and the band used for quantification is shown at the arrowhead in each case. Histograms show the mean and standard error of ROD readings across multiple membranes (n = 3 to 4) normalized to actin as loading control. (*P < 0.05, **P ≤ 0.01, ***P ≤ 0.001 NK).

filaments under the conditions studied. IL-6 was also a positive regulator of its own expression in astrocytes, inducing 2.4-fold higher levels relative to cultures treated with vehicle alone ($P = 0.02$, Student t-test). In addition, IL-6 promoted a 330-fold increase in PAR2 expression and a 2.5-fold increase in the expression of its agonist neurosin ($P \leq 0.01$, Student t-test).

3.7. Neurosin-PAR2 driven IL-6 secretion involves STAT3 and ERK1/2 signal transduction pathways

A combination of astrocytes derived from wild type or PAR2 −/− mice, the SCI-relevant PAR2 agonist neurosin (150 nM), and small molecule inhibitors of STAT3 (Stattic, 5 or 20 μm) or MEK1/2 (U0126, 150 μM) signaling, were used to examine the potential mechanism by which PAR2 elicits IL-6 secretion in primary astrocytes. MEK1/2 was chosen for study as an inhibitor of extracellular-signal-regulated kinase (ERK1/2), a signaling intermediate activated by PAR2 (DeFea et al., 2000), including astrocyte PAR2 (Vandell et al., 2008; McCoy et al., 2011). STAT3 was chosen for study because of its well known action in IL-6 signaling, although it is not known to signal directly downstream of GPCRs such as PAR2. Neurosin promoted consistent IL-6 secretion, ranging from 1.5- to greater than 3-fold elevations after 24 h ($P < 0.001$, Student t-test, Fig. 8A, D, E). Neurosin-induced IL-6 secretion was reduced by 2-fold, but not eliminated, in astrocytes lacking PAR2 ($P < 0.001$, Student t-test, Fig. 8A). The ability of neurosin to also signal through PAR1 in astrocytes to elicit IL-6 secretion (Vandell et al., 2008; Scarisbrick et al., 2012a, 2012b) may account for neurosin-IL-6 secretion, albeit at lower levels, even in the absence of PAR2. Examination of STAT3 signaling in the same neurosin-treated cultures demonstrated that neurosin promoted a 1.8-fold elevation in pSTAT3 and a 1.3-fold elevation in total STAT3 ($P \leq 0.04$, Student t-test), increases that were eliminated in astrocytes lacking PAR2 (Fig. 8B and C). Neurosin-mediated IL-6 secretion was also reduced by a STAT3-specific inhibitor ($P = 0.01$, Fig. 8D), or by a small molecule inhibitor of MEK1/2 ($P < 0.001$, Student t-test, Fig. 8E). Taken together, these data suggest a model in which neurosin can elicit IL-6 secretion by activating PAR2

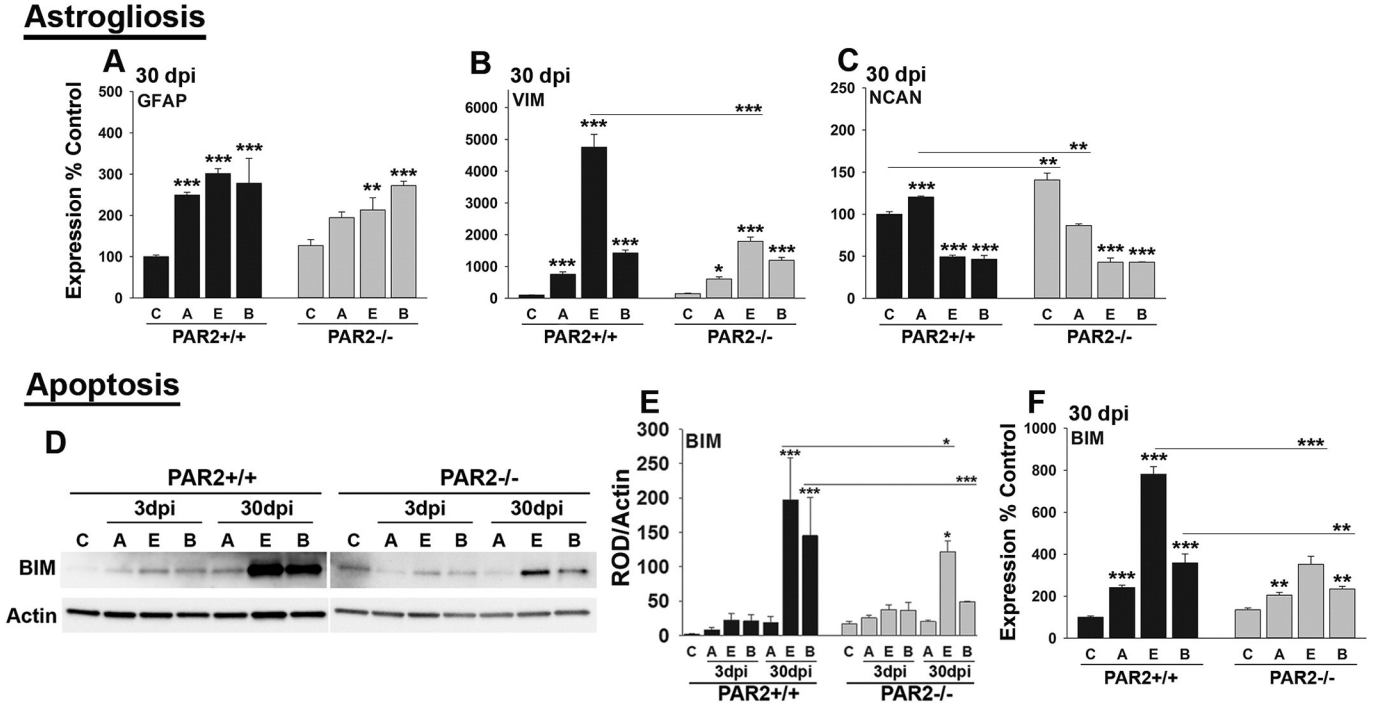

Fig. 5. Spinal cord injury-induced elevations in markers of astrogliosis and apoptosis were reduced in mice lacking the PAR2 gene. Histograms show transcriptional changes in RNA encoding GFAP (A), vimentin (VIM, (B)), neurocan (NCAN, (C)), and BIM (F) in the spinal cord of PAR2 +/+ or PAR2 −/− uninjured controls (C), or in the 3 mm of spinal cord surrounding the injury epicenter (E), or that above (A), or below (B), at 30 dpi. The RNA expression levels shown are expressed as a percent of the uninjured genotype control and these data were used for statistical comparisons. In addition, to facilitate interpretation of any impact of PAR2 gene deletion on gene expression in the uninjured spinal cord, and to permit statistical comparisons, expression levels shown for uninjured control PAR2 −/− mice are expressed as a percent of uninjured PAR2 +/+ controls. Baseline levels of neurocan were higher in PAR2 −/− compared to PAR2 +/+ mice. Western blots (D) and corresponding histogram (E) show that elevations in the pro-apoptotic protein BIM observed at 30 dpi were significantly attenuated in mice lacking PAR2. (*P < 0.05, **P ≤ 0.01, ***P ≤ 0.001 NK).

and that the intracellular pathways involved likely include both MEK1/2 and STAT3 signaling mechanisms (Fig. 9). In this suggested model, neurosin-PAR2-mediated IL-6 secretion feeds forward to activate STAT3 signaling by activation of the IL-6 receptor. The STAT3 transcription factor in turn drives expression of GFAP, vimentin, and additional IL-6. In addition, our findings suggest that IL-6-STAT3 signaling drives

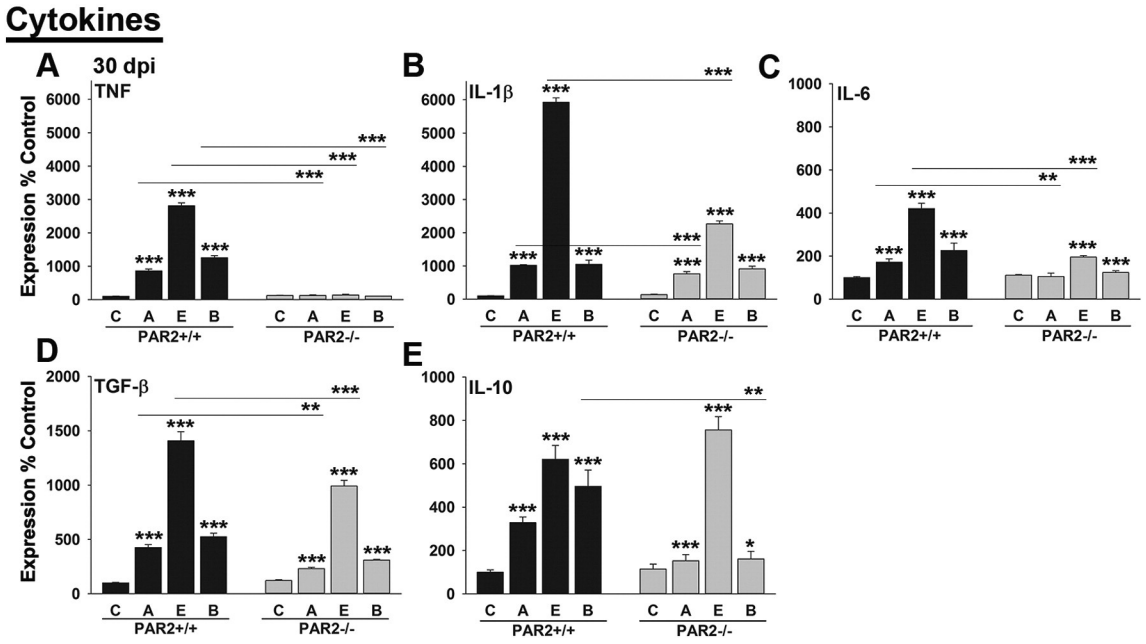

Fig. 6. Spinal cord injury-induced elevations in pro-inflammatory cytokines were reduced in mice lacking the PAR2 gene. Histograms show transcriptional changes in RNA encoding pro-inflammatory (TNF, IL1-β, IL-6), or anti-inflammatory cytokines (TGF-β, IL-10), in the spinal cord of PAR2 +/+ or PAR2 −/− uninjured controls (C), or in the 3 mm of spinal cord surrounding the injury epicenter (E), or that above (A), or below (B), at 30 dpi. The RNA expression levels shown are expressed as a percent of the uninjured genotype control and these data were used for statistical comparisons. In addition, to facilitate interpretation of any impact of PAR2 gene deletion on cytokine expression in the uninjured spinal cord, and to permit statistical comparisons, expression levels shown for uninjured control PAR2 −/− mice are expressed as a percent of uninjured PAR2 +/+ controls. No significant differences in cytokine RNA expression were observed in the uninjured spinal cord between PAR2 +/+ and PAR2 −/− mice. (*P < 0.05, **P ≤ 0.01, ***P ≤ 0.001 NK).

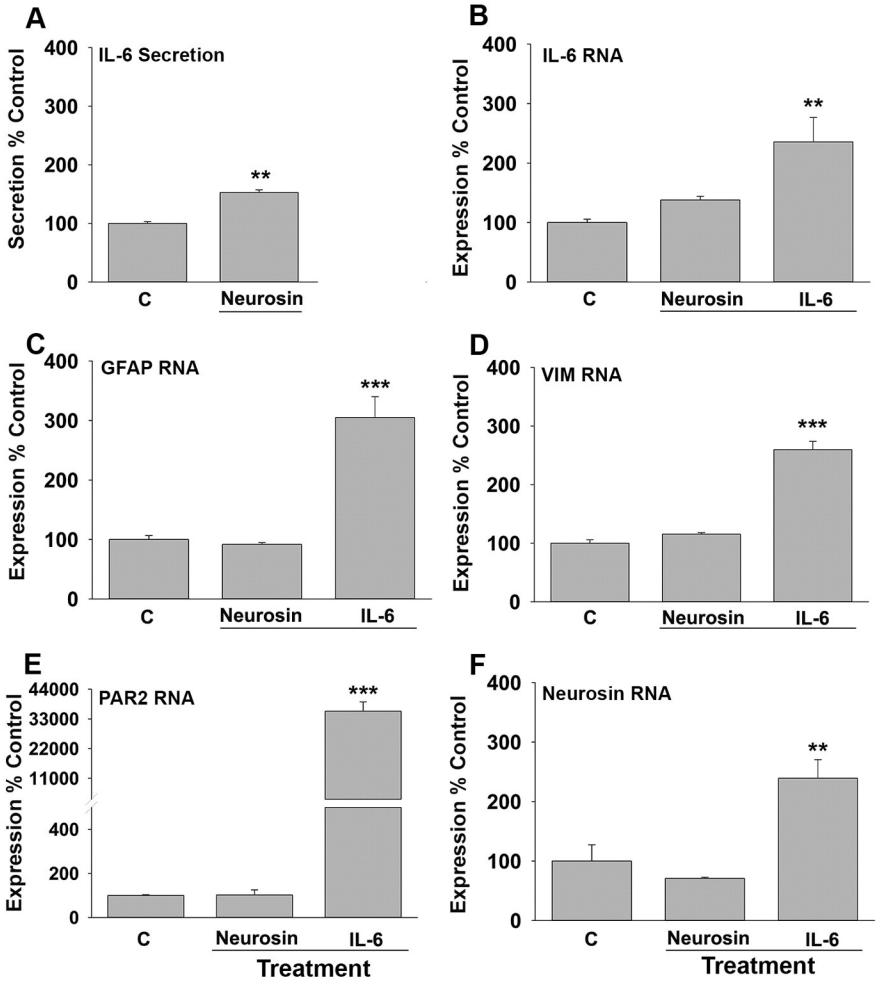

Fig. 7. IL-6 is a positive driver of astroglial intermediate filament proteins and the PAR2-signaling axis in primary astrocytes. (A) Treatment of astrocytes with neurosin (150 ng/ml) for 24 h resulted in a significant increase in IL-6 secretion. (B) Astrocyte cultures treated with recombinant IL-6 (20 ng/ml) showed increased IL-6 RNA expression. Recombinant IL-6 also promoted significant increases in the expression of GFAP (C), vimentin (D), PAR2 (E), and neurosin (F) RNA. (*$P < 0.05$, **$P \leq 0.01$, ***$P \leq 0.001$, Students t-test).

elevations in both PAR2 and neurosin, therefore feeding back to create a potentially cyclical signaling circuit that ultimately serves to intensify the process of inflammatory-astrogliosis.

4. Discussion

The results presented suggest that PAR2 can serve as an extracellular switch turning on signaling after SCI that limits motor recovery at least in part by promoting inflammation and astrogliosis. *In vivo* and *in vitro* findings are presented which support a model in which PAR2 activation promotes IL-6-STAT3 signaling and contributes to pro-inflammatory cytokine production and astroglial scar formation through serial feedforward and feedback signaling mechanisms. Evidence further suggests that this biological signaling node offers tangible therapeutic potential for SCI since global PAR2 deletion results in significant improvements in motor recovery and reduced signs of inflammation, astrogliosis, and axon degeneration.

This is the first report that PAR2 activation is an essential mediator of inflammation, astrogliosis and functional decline in SCI. PAR2 has been linked to other neuropathologies, although its primarily detrimental or beneficial actions are equivocal with outcomes pathology-related. The current findings suggest that in spinal cord trauma, PAR2-activation has a deleterious impact on neurobehavioral outcomes and that this is linked in part to PAR2-driven inflammation and astrogliosis. For example, SCI-elicited increases in molecular signatures of astrogliosis, namely the intermediate filament proteins GFAP and vimentin, and the neurite outgrowth inhibitory protein neurocan (Laabs et al., 2007), were all substantially lower in mice lacking PAR2. Also, SCI-associated elevations in pro-inflammatory cytokines namely TNF (Kim et al., 2001), IL-1β (Wang et al., 2005), and IL-6 (Okada et al., 2004), known to be produced by immune cells and activated astrocytes and to mediate neural injury responses, were also reduced in mice lacking PAR2. Indeed, in PAR2 −/− mice there was a complete absence of elevations in TNF evident at 30 dpi in the wild type injured spinal cord. IL-10 is primarily produced by monocytes (Pestka et al., 2004) and reduced levels in the PAR2 −/− injured spinal cord below the level of injury may reflect reductions in microglial/macrophage infiltration observed at the same lesion level immunopathologically (Letterio and Roberts, 1998). In conjunction with reductions in pro-inflammatory cytokines, substantial reductions in SCI-induced expression of the pro-apoptotic signaling protein BIM, and increases in PKCγ-immunoreactivity, a marker of corticospinal axon functional status (Lieu et al., 2013), were also observed after SCI in PAR2 deficient mice (Laabs et al., 2007). While additional studies using cell specific PAR2 −/− knockdown strategies will be needed to address whether the reductions in pro-inflammatory cytokines and astrogliosis and the improved functional status of corticospinal axons observed in PAR2 −/− mice may occur by direct or indirect means, it is likely that these changes collectively contributed to the improvements in motor outcomes observed.

The elevations in PAR2 expression in response to traumatic SCI observed at early and chronic time points position this GPCR to exert fundamental actions in the cascade of events occurring secondary to spinal

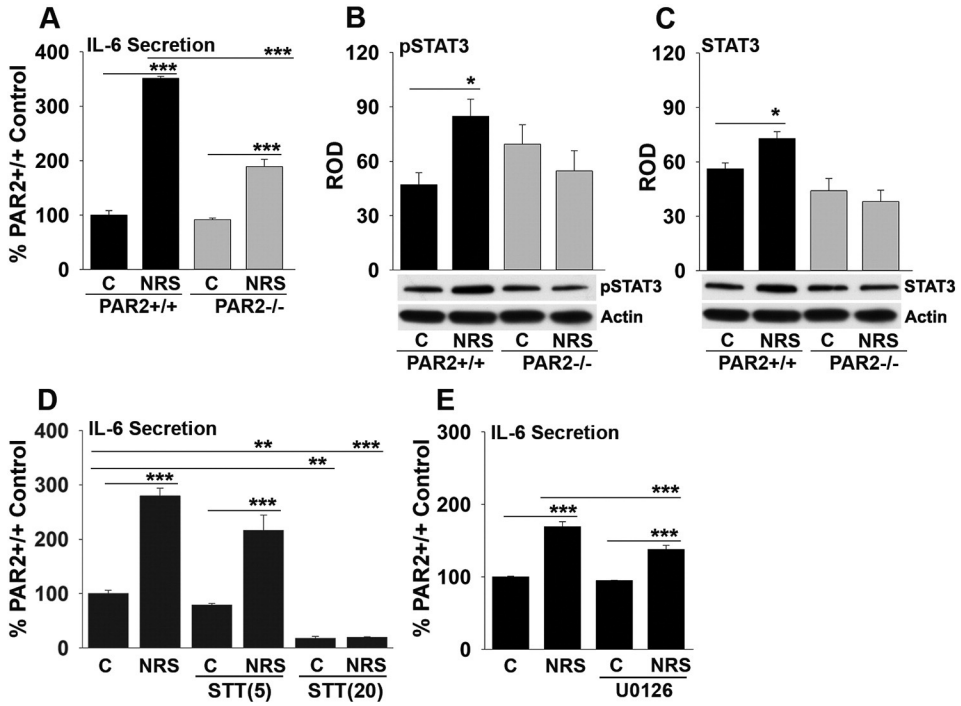

Fig. 8. PAR2-neurosin dependent mechanism of IL-6 secretion in primary astrocytes. (A) Neurosin (NRS), (150 nM, 24 h)-mediated IL-6 secretion is reduced in astrocytes derived from PAR2 knockout mice. Neurosin also stimulates increases in pSTAT3 (B), and total STAT3 (C), and these signaling responses were blocked in astrocytes lacking PAR2. A small molecule inhibitor of STAT3 (Stattic, 5 or 20 μM), or of MEK1/2 (U0126, 150 μM), each significantly attenuated neurosin-mediated IL-6 secretion (D, E). IL-6 secretion was measured by ELISA in cell culture supernatants. (*P < 0.05, **P ≤ 0.01, ***P ≤ 0.001 NK).

trauma. Additionally, neurosin (Klk6), a newly recognized CNS-endogenous agonist of PAR2 (Vandell et al., 2008; Yoon et al., 2013), was elevated in a coordinate manner, and is therefore positioned to serve as a major activator of PAR2 after SCI. Neurosin has been previously implicated in SCI, with elevations occurring in experimental models (Scarisbrick et al., 1997, 2006b; Terayama et al., 2004; Yoon et al., 2013) and in human SCI, persisting as long as 5 years post-injury (Scarisbrick et al., 2006b; Radulovic et al., 2013). Supporting a role for neurosin in inflammatory astrogliosis, it is up regulated in astrocytes and localized to macrophages/microglia in the context of SCI and in actively demyelinating MS plaques (Scarisbrick et al., 1997, 2002, 2006b, 2012a; Blaber et al., 2004). Here we verify the up regulation of neurosin in GFAP+ astrocytes within the spinal cord at 30 dpi and demonstrate that PAR2 is elevated in astrocytes in a parallel manner. In addition, *in vitro* studies demonstrate that excess neurosin promotes injury to neurons (Scarisbrick et al., 2008; Yoon et al., 2013), to myelin and myelinating oligodendrocytes (Scarisbrick et al., 2002; Burda et al., 2013), and drives key features of astrogliosis, including astrocyte stellation and IL-6 secretion (Scarisbrick et al., 2012a). Emerging data indicate neurosin exerts multiple physiologic actions relevant to SCI pathogenesis, including attenuating immune cell apoptosis (Scarisbrick et al., 2011), and driving innate and adaptive immune responses (Scarisbrick et al., 2006a, 2012b; Panos et al., 2014). These prior studies, taken with current findings that SCI-induced elevations in neurosin are reduced in the absence of PAR2, leave open the possibility that improvements in sensorimotor outcomes in PAR2-deficient mice may be linked in part to reduced elevations in this potent PAR2 agonist. Since the current studies point to a key role of IL-6 in promoting neurosin expression by astrocytes, it is possible that the reductions in IL-6 in the spinal cord of PAR2 −/− mice after SCI may underlie at least in part the coordinate reductions in neurosin observed.

A systematic investigation of the molecular profile of SCI in PAR2 +/+ and PAR2 −/− mice, points to a mechanistic link between PAR2 and canonical IL-6-STAT3-signaling. Molecular profiling of the SCI epicenter and segments above and below indicates that mice lacking PAR2 show significantly reduced STAT3 signaling after SCI as well as reductions in the STAT3 activator, IL-6. Since STAT3 is a well-established mediator of IL-6-driven astrogliosis in SCI (Okada et al., 2006; Herrmann et al., 2008), it is possible that reductions in SCI-associated IL-6 and STAT3 signaling observed in PAR2 −/− mice may have contributed to the reductions in astrogliosis and improved neurobehavioral outcomes observed. Importantly in this regard, conditional deletion of STAT3 in astrocytes significantly attenuates astroglial scar formation after SCI (Okada et al., 2006; Herrmann et al., 2008; Wanner et al., 2013). However, targeting astrocyte STAT3 alone also resulted in an increase in inflammation and lesion size and overall reduced motor recovery establishing for the first time the key role of astrocytes in controlling injury associated inflammatory and wound healing responses. By contrast, we show that genetic deletion of PAR2 globally not only promotes reductions in SCI-elicited astrogliosis, but also results in reductions in other pro-inflammatory cytokines, including TNF and IL1-β, as well as reductions in microglia/monocytes. It is likely therefore that the significant neurobehavioral improvements seen in PAR2 −/− mice after SCI reflect the combined impact of deleting PAR2 on pro-inflammatory responses, in addition to effects on attenuating astrogliosis. It is also important to point out that the wound healing response in SCI is complex. IL-6 not only contributes to astrogliosis, but also may promote direct nerve injury (Kaplin et al., 2005) or repair in certain conditions (Cafferty et al., 2004; Yang et al., 2012; Lang et al., 2013). It will be highly valuable in future studies to determine how targeting PAR2 selectively in the different cell types involved in the response of the spinal cord to traumatic injury, including astrocytes, microglia, oligodendrocytes and neurons, affects cellular, molecular and behavioral recovery to shed further light on the mechanism of action of this receptor and its potential therapeutic utility.

To begin to deconstruct the nature of PAR2-mediated astroglial activation and the emerging relationship that our data suggest exists between PAR2, IL-6, and STAT3-signaling, we evaluated the ability of the SCI relevant PAR2 agonist neurosin (Scarisbrick et al., 1997, 2006b; Radulovic et al., 2013; Yoon et al., 2013) to drive hallmarks of astrogliosis in primary astrocytes *in vitro*. Neurosin increased both IL-6

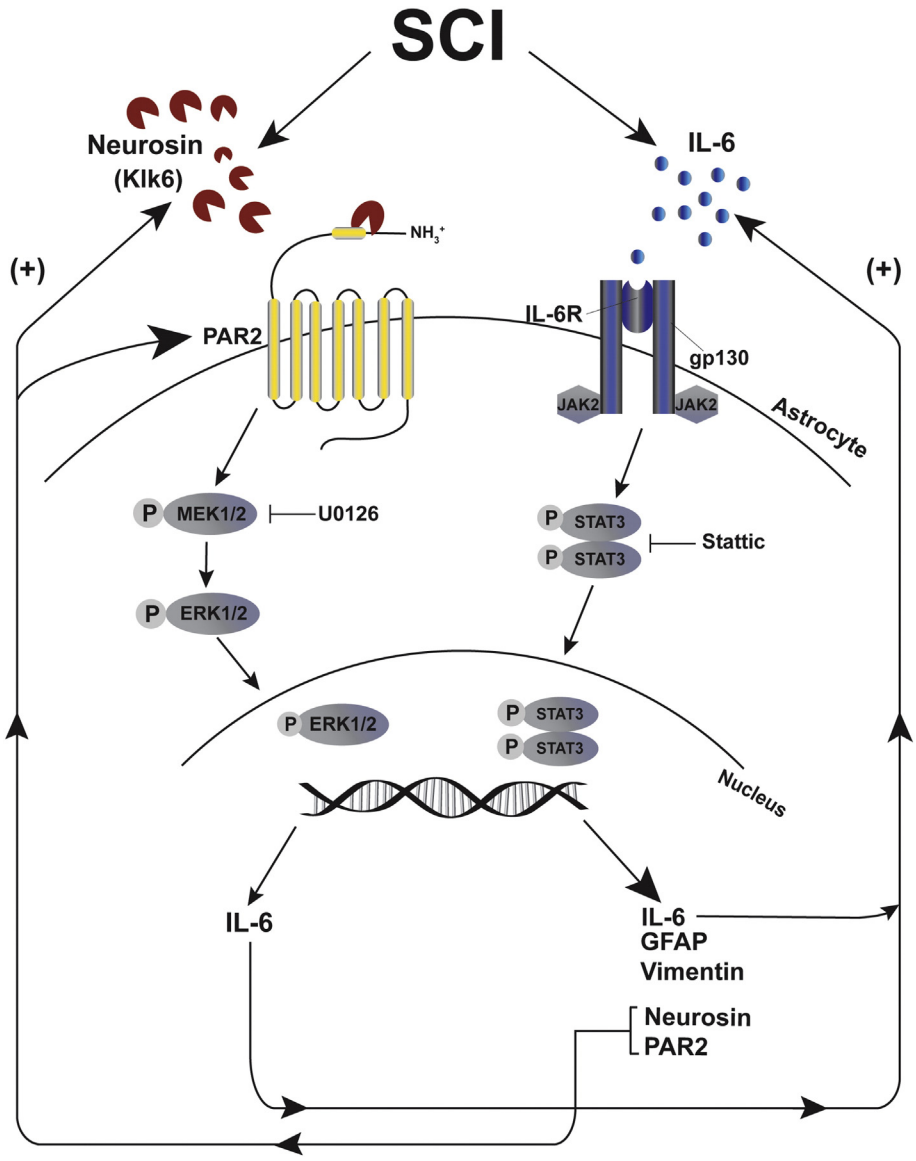

Fig. 9. Model depicting how activation of PAR2 in astrocytes may promote IL-6-mediated STAT3 signaling and astrogliosis. Data presented suggest that SCI promotes elevations in PAR2 and its CNS endogenous agonist neurosin (Klk6). Prior studies demonstrate that neurosin is produced by reactive astrocytes and activated microglia/macrophages at sites of spinal cord trauma (Scarisbrick et al., 2006b, 2012a; Radulovic et al., 2013). Neurosin cleaves thereby activating PAR2 (Vandell et al., 2008) to elicit IL-6 secretion at least in part by a MEK1/2-dependent signaling mechanism. Astrocyte derived IL-6, along with that generated by immune cells at sites of SCI is a well studied activator of STAT3 signaling (Darnell, 1997) and elicits expression of GFAP, vimentin (VIM) and additional IL-6 in primary astrocyte cultures. Data presented also suggest that IL-6 can increase expression of PAR2 (330-fold) and neurosin (2.5-fold) thereby contributing to a reverberating signaling circuit in astrocytes that will ultimately promote astrogliosis.

secretion and STAT3 signaling in cultures of primary astrocytes in a PAR2-dependent manner. Treatment of astrocytes with neurosin for 24 h consistently produced increases in IL-6 secretion, although clear elevations in other hallmarks of astrogliosis, namely the expression of the intermediate filament proteins GFAP and vimentin, were not repeatedly observed. In turn, recombinant IL-6 increased neurosin expression by 2.5-fold. IL-6 was also a vigorous activator of GFAP, vimentin, and IL-6 expression, a finding consistent with the established role of this pro-inflammatory cytokine as a powerful mediator of astrogliosis (Klein et al., 1997; Okada et al., 2004). Results therefore suggest that *in vitro*, neurosin modulates astroglial responses by promoting astrocyte IL-6 secretion rather than driving robust changes in GFAP. It will be important to address the effects of other PAR2 agonists relevant to SCI, including kallikreins 5, 7 and 9 (Radulovic et al., 2013), to further define the ability of PAR2 to directly modulate GFAP expression *in vitro* and *in vivo*. Interestingly, data presented suggest that activation of PAR2 not only increases astrocyte IL-6 secretion, but also that IL-6 is a potent regulator of astrocyte PAR2 increasing expression of this receptor by 330-fold. It is possible that interruption of the reciprocal regulatory interactions between PAR2 and IL-6 in PAR2 −/− mice after SCI contributes to the reductions in markers of astrogliosis observed, including GFAP, vimentin and IL-6, in addition to STAT3 signaling. Together, the current findings point to the need to fully delineate the spectrum of PAR2 agonists operative in SCI and their potential downstream actions.

While neurosin was shown to promote activation of STAT3 in a PAR2 dependent manner, there is little evidence that this can occur directly. GPCRs such as PAR2 have not been directly linked to activation of STAT3, and indeed any direct link has been shown to be inhibitory (Chung et al., 1997; Sengupta et al., 1998). An alternative possibility is that PAR2 activates STAT3 indirectly by way of its ability to promote secretion of the canonical STAT3 activator IL-6. PAR2 is a well-established activator of mitogen-activated protein kinase (MAPKs) signaling cascades, including ERK1/2 in astrocytes (Wang et al., 2002; Vandell et al., 2008; McCoy et al., 2011). Experiments here indicate that PAR2 signaling through ERK1/2 may play a role in PAR2-mediated IL-6 secretion since a small molecule inhibitor of this signaling

pathway significantly reduces neurosin-mediated IL-6 secretion (Wang et al., 2002; Vandell et al., 2008; McCoy et al., 2011). In turn, IL-6 is known to drive markers of astrogliosis, including additional IL-6 expression and here we show that STAT3 inhibition also reduces neurosin-mediated IL-6 secretion in a dose dependent manner. Of interest, like STAT3 (Herrmann et al., 2008; Wanner et al., 2013), prior studies also point to a critical role for ERK1/2 signaling in SCI-induced astrogliosis (Lu et al., 2010; Lin et al., 2014). Together these findings suggest that SCI-induced IL-6 can serve as an integrator of the ERK1/2 and STAT3 signal transduction pathways driving key facets of astrogliosis. The limited ability of the PAR2 agonist neurosin to promote robust increases in GFAP or vimentin expression on its own, as would be expected if direct STAT3 activation were involved, also supports the idea that an indirect mechanism of PAR2-STAT3 activation in astrocytes likely predominates. Since PAR2 gene deletion was shown to dramatically reduce STAT3 signaling in the context of SCI, the current studies provide important rationale to further dissect the signaling intermediate(s) involved.

5. Conclusion

Given the key role of IL-6 in promoting astrogliosis (Okada et al., 2004), including expression of GFAP and vimentin, we propose a model whereby proteases unleashed after SCI, such as neurosin, contribute to pathogenesis and suppress repair at least in part by their ability to switch on a PAR2-IL-6-STAT3 signaling cascade that promotes inflammatory astroglial responses. Our findings suggest that therapies targeting PAR2 signaling globally may prove useful to limit trauma-induced astrogliosis, to constrain pro-inflammatory cytokine production and apoptosis, and to protect sparred axons. Future studies are needed to define the range of cells expressing PAR2 in SCI and to determine essential mechanisms involved by selective targeting of PAR2 in different cell types. In addition, to move this research towards clinical translation, it will be necessary to determine whether PAR2-inhibitors, applied at select time points after injury, replicate or enhance the improvements in functional outcomes observed here in the case of global PAR2 gene deletion.

Conflict of interest

The authors declare no competing financial interests.

Acknowledgments

Studies were supported by the National Institutes of Health 5R01NS052741, Pilot Project PP2009 and a Collaborative MS Research Center Award CA1060A11 from the National Multiple Sclerosis Society, and an Accelerated Regenerative Medicine Award from the Mayo Clinic Center for Regenerative Medicine. The authors declare no competing financial interests.

References

Asher, R.A., Morgenstern, D.A., Moon, L.D., Fawcett, J.W., 2001. Chondroitin sulphate proteoglycans: inhibitory components of the glial scar. Prog. Brain Res. 132, 611–619.
Basso, D.M., Fisher, L.C., Anderson, A.J., Jakeman, L.B., McTigue, D.M., Popovich, P.G., 2006. Basso mouse scale for locomotion detects differences in recovery after spinal cord injury in five common mouse strains. J. Neurotrauma 23, 635–659.
Bastien, D., Lacroix, S., 2014. Cytokine pathways regulating glial and leukocyte function after spinal cord and peripheral nerve injury. Exp. Neurol. 258, 62–77.
Blaber, S.I., Ciric, B., Christophi, G.P., Bernett, M.J., Blaber, M., Rodriguez, M., Scarisbrick, I.A., 2004. Targeting kallikrein 6-proteolysis attenuates CNS inflammatory disease. FASEB J. 19, 920–922.
Bradbury, E.J., Moon, L.D., Popat, R.J., King, V.R., Bennett, G.S., Patel, P.N., Fawcett, J.W., McMahon, S.B., 2002. Chondroitinase ABC promotes functional recovery after spinal cord injury. Nature 416, 636–640.
Burda, J.E., Radulovic, M., Yoon, H., Scarisbrick, I.A., 2013. Critical role for PAR1 in kallikrein 6-mediated oligodendrogliopathy. Glia 61, 1456–1470.
Cafferty, W.B., Gardiner, N.J., Das, P., Qiu, J., McMahon, S.B., Thompson, S.W., 2004. Conditioning injury-induced spinal axon regeneration fails in interleukin-6 knock-out mice. J. Neurosci. 24, 4432–4443.
Chung, J., Uchida, E., Grammer, T.C., Blenis, J., 1997. STAT3 serine phosphorylation by ERK-dependent and -independent pathways negatively modulates its tyrosine phosphorylation. Mol. Cell. Biol. 17, 6508–6516.
Cummings, B.J., Engesser-Cesar, C., Cadena, G., Anderson, A.J., 2007. Adaptation of a ladder beam walking task to assess locomotor recovery in mice following spinal cord injury. Behav. Brain Res. 177, 232–241.
Darnell Jr., J.E., 1997. STATs and gene regulation. Science 277, 1630–1635.
DeFea, K.A., Zalevsky, J., Thoma, M.S., Dery, O., Mullins, R.D., Bunnett, N.W., 2000. beta-arrestin-dependent endocytosis of proteinase-activated receptor 2 is required for intracellular targeting of activated ERK1/2. J. Cell Biol. 148, 1267–1281.
Dominguez, E., Mauborgne, A., Mallet, J., Desclaux, M., Pohl, M., 2010. SOCS3-mediated blockade of JAK/STAT3 signaling pathway reveals its major contribution to spinal cord neuroinflammation and mechanical allodynia after peripheral nerve injury. J. Neurosci. 30, 5754–5766.
Ferrell, W.R., Lockhart, J.C., Kelso, E.B., Dunning, L., Plevin, R., Meek, S.E., Smith, A.J., Hunter, G.D., McLean, J.S., McGarry, F., Ramage, R., Jiang, L., Kanke, T., Kawagoe, J., 2003. Essential role for proteinase-activated receptor-2 in arthritis. J. Clin. Invest. 111, 35–41.
Gan, J., Greenwood, S.M., Cobb, S.R., Bushell, T.J., 2011. Indirect modulation of neuronal excitability and synaptic transmission in the hippocampus by activation of proteinase-activated receptor-2. Br. J. Pharmacol. 163, 984–994.
Herrmann, J.E., Imura, T., Song, B., Qi, J., Ao, Y., Nguyen, T.K., Korsak, R.A., Takeda, K., Akira, S., Sofroniew, M.V., 2008. STAT3 is a critical regulator of astrogliosis and scar formation after spinal cord injury. J. Neurosci. 28, 7231–7243.
Jin, G., Hayashi, T., Kawagoe, J., Takizawa, T., Nagata, T., Nagano, I., Syoji, M., Abe, K., 2005. Deficiency of PAR-2 gene increases acute focal ischemic brain injury. J. Cereb. Blood Flow Metab. 25, 302–313.
Joshi, M., Fehlings, M., 2002a. Development and characterization of a novel, graded model of clip compressive spinal cord injury in the mouse: Part 2. Quantitative neuroanatomical assessment and analysis of the relationships between axonal tracts, residual tissue, and locomotor recovery. J. Neurotrauma 19, 191–203.
Joshi, M., Fehlings, M., 2002b. Development and characterization of a novel, graded model of clip compressive spinal cord injury in the mouse: Part 1. Clip design, behavioral outcomes, and histopathology. J. Neurotrauma 19, 175–190.
Kaplin, A.I., Deshpande, D.M., Scott, E., Krishnan, C., Carmen, J.S., Shats, I., Martinez, T., Drummond, J., Dike, S., Pletnikov, M., Keswani, S.C., Moran, T.H., Pardo, C.A., Calabresi, P.A., Kerr, D.A., 2005. IL-6 induces regionally selective spinal cord injury in patients with the neuroinflammatory disorder transverse myelitis. J. Clin. Invest. 115, 2731–2741.
Karimi-Abdolrezaee, S., Eftekharpour, E., Wang, J., Schut, D., Fehlings, M.G., 2010. Synergistic effects of transplanted adult neural stem/progenitor cells, chondroitinase, and growth factors promote functional repair and plasticity of the chronically injured spinal cord. J. Neurosci. 30, 1657–1676.
Kawagoe, J., Takizawa, T., Matsumoto, J., Tamiya, M., Meek, S.E., Smith, A.J., Hunter, G.D., Pelvin, R., Saito, N., Kanke, T., Fujii, M., Wada, Y., 2002. Effect of protease-activated receptor-2 deficiency on allergic dermatitis in the mouse ear. Jpn. J. Pharmacol. 88, 77–84.
Kendziorski, C., Irizarry, R.A., Chen, K.S., Haag, J.D., Gould, M.N., 2005. On the utility of pooling biological samples in microarray experiments. Proc. Natl. Acad. Sci. U. S. A. 102, 4252–4257.
Kim, G.M., Xu, J., Xu, J., Song, S.K., Yan, P., Ku, G., Xu, X.M., Hsu, C.Y., 2001. Tumor necrosis factor receptor deletion reduces nuclear factor-kappaB activation, cellular inhibitor of apoptosis protein 2 expression, and functional recovery after traumatic spinal cord injury. J. Neurosci. 21, 6617–6625.
Kim, O.S., Park, E.J., Joe, E.H., Jou, I., 2002. JAK-STAT signaling mediates gangliosides-induced inflammatory responses in brain microglial cells. J. Biol. Chem. 277, 40594–40601.
Klein, M.A., Moller, J.C., Jones, L.L., Bluethmann, H., Kreutzberg, G.W., Raivich, G., 1997. Impaired neuroglial activation in interleukin-6 deficient mice. Glia 19, 227–233.
Klusman, I., Schwab, M.E., 1997. Effects of pro-inflammatory cytokines in experimental spinal cord injury. Brain Res. 762, 173–184.
Kouzaki, H., O'Grady, S.M., Lawrence, C.B., Kita, H., 2009. Proteases induce production of thymic stromal lymphopoietin by airway epithelial cells through protease-activated receptor-2. J. Immunol. 183, 1427–1434.
Laabs, T.L., Wang, H., Katagiri, Y., McCann, T., Fawcett, J.W., Geller, H.M., 2007. Inhibiting glycosaminoglycan chain polymerization decreases the inhibitory activity of astrocyte-derived chondroitin sulfate proteoglycans. J. Neurosci. 27, 14494–14501.
Lang, C., Bradley, P.M., Jacobi, A., Kerschensteiner, M., Bareyre, F.M., 2013. STAT3 promotes corticospinal remodelling and functional recovery after spinal cord injury. EMBO Rep. 14, 931–937.
Lepekhin, E.A., Eliasson, C., Berthold, C.H., Berezin, V., Bock, E., Pekny, M., 2001. Intermediate filaments regulate astrocyte motility. J. Neurochem. 79, 617–625.
Letterio, J.J., Roberts, A.B., 1998. Regulation of immune responses by TGF-beta. Annu. Rev. Immunol. 16, 137–161.
Lieu, A., Tenorio, G., Kerr, B.J., 2013. Protein kinase C gamma (PKCgamma) as a novel marker to assess the functional status of the corticospinal tract in experimental autoimmune encephalomyelitis (EAE). J. Neuroimmunol. 256, 43–48.
Lin, B., Xu, Y., Zhang, B., He, Y., Yan, Y., He, M.C., 2014. MEK inhibition reduces glial scar formation and promotes the recovery of sensorimotor function in rats following spinal cord injury. Exp. Ther. Med. 7, 66–72.
Lu, K., Liang, C.L., Liliang, P.C., Yang, C.H., Cho, C.L., Weng, H.C., Tsai, Y.D., Wang, K.W., Chen, H.J., 2010. Inhibition of extracellular signal-regulated kinases 1/2 provides neuroprotection in spinal cord ischemia/reperfusion injury in rats: relationship with the nuclear factor-kappaB-regulated anti-apoptotic mechanisms. J. Neurochem. 114, 237–246.
Luo, W., Wang, Y., Reiser, G., 2007. Protease-activated receptors in the brain: receptor expression, activation, and functions in neurodegeneration and neuroprotection. Brain Res. Rev. 56, 331–345.

McCoy, K.L., Traynelis, S.F., Hepler, J.R., 2011. PAR1 and PAR2 couple to overlapping and distinct sets of G proteins and linked signaling pathways to differentially regulate cell physiology. Mol. Pharmacol. 77, 1005–1015.
Mori, M., Kose, A., Tsujino, T., Tanaka, C., 1990. Immunocytochemical localization of protein kinase C subspecies in the rat spinal cord: light and electron microscopic study. J. Comp. Neurol. 299, 167–177.
Noorbakhsh, F., Vergnolle, N., McArthur, J.C., Silva, C., Vodjgani, M., Andrade-Gordon, P., Hollenberg, M.D., Power, C., 2005. Proteinase-activated receptor-2 induction by neuroinflammation prevents neuronal death during HIV infection. J. Immunol. 174, 7320–7329.
Noorbakhsh, F., Tsutsui, S., Vergnolle, N., Boven, L.A., Shariat, N., Vodjgani, M., Warren, K.G., Andrade-Gordon, P., Hollenberg, M.D., Power, C., 2006. Proteinase-activated receptor 2 modulates neuroinflammation in experimental autoimmune encephalomyelitis and multiple sclerosis. J. Exp. Med. 203, 425–435.
Okada, S., Nakamura, M., Mikami, Y., Shimazaki, T., Mihara, M., Ohsugi, Y., Iwamoto, Y., Yoshizaki, K., Kishimoto, T., Toyama, Y., Okano, H., 2004. Blockade of interleukin-6 receptor suppresses reactive astrogliosis and ameliorates functional recovery in experimental spinal cord injury. J. Neurosci. Res. 76, 265–276.
Okada, S., Nakamura, M., Katoh, H., Miyao, T., Shimazaki, T., Ishii, K., Yamane, J., Yoshimura, A., Iwamoto, Y., Toyama, Y., Okano, H., 2006. Conditional ablation of Stat3 or Socs3 discloses a dual role for reactive astrocytes after spinal cord injury. Nat. Med. 12, 829–834.
Panos, M., Christophi, G.P., Rodriguez, M., Scarisbrick, I.A., 2014. Differential expression of multiple kallikreins in a viral model of multiple sclerosis points to unique roles in the innate and adaptive immune response. Biol. Chem. 395, 1063–1073.
Pekny, M., Pekna, M., 2004. Astrocyte intermediate filaments in CNS pathologies and regeneration. J. Pathol. 204, 428–437.
Pekny, M., Eliasson, C., Siushansian, R., Ding, M., Dixon, S.J., Pekna, M., Wilson, J.X., Hamberger, A., 1999. The impact of genetic removal of GFAP and/or vimentin on glutamine levels and transport of glucose and ascorbate in astrocytes. Neurochem. Res. 24, 1357–1362.
Pestka, S., Krause, C.D., Sarkar, D., Walter, M.R., Shi, Y., Fisher, P.B., 2004. Interleukin-10 and related cytokines and receptors. Annu. Rev. Immunol. 22, 929–979.
Radulovic, M., Yoon, H., Larson, N., Wu, J., Linbo, R., Burda, J.E., Diamandis, E.P., Blaber, S.I., Blaber, M., Fehlings, M.G., Scarisbrick, I.A., 2013. Kallikrein cascades in traumatic spinal cord injury: in vitro evidence for roles in axonopathy and neuron degeneration. J. Neuropathol. Exp. Neurol. 72, 1072–1089.
Ramachandran, R., Noorbakhsh, F., Defea, K., Hollenberg, M.D., 2012. Targeting proteinase-activated receptors: therapeutic potential and challenges. Nat. Rev. Drug Discov. 11, 69–86.
Scarisbrick, I.A., Blaber, M., 2012. Kallikrein-related peptidase 6. In: Barrett, A.J., Rawlings, N.D. (Eds.), Handbook of Proteolytic Enzymes, 3rd edition, pp. 2780–2786.
Scarisbrick, I.A., Towner, M.D., Isackson, P.J., 1997. Nervous system specific expression of a novel serine protease: regulation in the adult rat spinal cord by excitotoxic injury. J. Neurosci. 17, 8156–8168.
Scarisbrick, I.A., Isackson, P.J., Windebank, A.J., 1999. Differential expression of brain-derived neurotrophic factor, neurotrophin-3, and neurotrophin-4/5 in the adult rat spinal cord: regulation by the glutamate receptor agonist kainic acid. J. Neurosci. 19, 7757–7769.
Scarisbrick, I.A., Blaber, S.I., Lucchinetti, C.F., Genain, C.P., Blaber, M., Rodriguez, M., 2002. Activity of a newly identified serine protease in CNS demyelination. Brain 125, 1283–1296.
Scarisbrick, I.A., Blaber, S.I., Tingling, J.T., Rodriguez, M., Blaber, M., Christophi, G.P., 2006a. Potential scope of action of tissue kallikreins in CNS immune-mediated disease. J. Neuroimmunol. 178, 167–176.
Scarisbrick, I.A., Sabharwal, P., Cruz, H., Larsen, N., Vandell, A., Blaber, S.I., Ameenuddin, S., Papke, L.M., Fehlings, M.G., Reeves, R.K., Blaber, M., Windebank, A.J., Rodriguez, M., 2006b. Dynamic role of kallikrein 6 in traumatic spinal cord injury. Eur. J. Neurosci. 24, 1457–1469.
Scarisbrick, I.A., Linbo, R., Vandell, A.G., Keegan, M., Blaber, S.I., Blaber, M., Sneve, D., Lucchinetti, C.F., Rodriguez, M., Diamandis, E.P., 2008. Kallikreins are associated with secondary progressive multiple sclerosis and promote neurodegeneration. Biol. Chem. 389, 739–745.
Scarisbrick, I.A., Epstein, B., Cloud, B.A., Yoon, H., Wu, J., Renner, D.N., Blaber, S.I., Blaber, M., Vandell, A.G., Bryson, A.L., 2011. Functional role of kallikrein 6 in regulating immune cell survival. PLoS One 6 (e18376) (18371-18311).
Scarisbrick, I.A., Radulovic, M., Burda, J.E., Larson, N., Blaber, S.I., Giannini, C., Blaber, M., Vandell, A.G., 2012a. Kallikrein 6 is a novel molecular trigger of reactive astrogliosis. Biol. Chem. 393, 355–367.
Scarisbrick, I.A., Yoon, H., Panos, M., Larson, N., Blaber, S.I., Blaber, M., Rodriguez, M., 2012b. Kallikrein 6 regulates early CNS demyelination in a viral model of multiple sclerosis. Brain Pathol. 22, 709–722.
Sengupta, T.K., Talbot, E.S., Scherle, P.A., Ivashkiv, L.B., 1998. Rapid inhibition of interleukin-6 signaling and Stat3 activation mediated by mitogen-activated protein kinases. Proc. Natl. Acad. Sci. U. S. A. 95, 11107–11112.
Silver, J., Miller, J.H., 2004. Regeneration beyond the glial scar. Nat. Rev. Neurosci. 5, 146–156.
Sofroniew, M.V., 2009. Molecular dissection of reactive astrogliosis and glial scar formation. Trends Neurosci. 32, 638–647.
Terayama, R., Bando, Y., Takahashi, T., Yoshida, S., 2004. Differential expression of neuropsin and protease M/neurosin in oligodendrocytes after injury to the spinal cord. Glia 48, 91–101.
Vandell, A.G., Larson, N., Laxmikanthan, G., Panos, M., Blaber, S.I., Blaber, M., Scarisbrick, I.A., 2008. Protease activated receptor dependent and independent signaling by Kallikreins 1 and 6 in CNS neuron and astroglial cell lines. J. Neurochem. 107, 855–870.
Vergnolle, N., Cellars, L., Mencarelli, A., Rizzo, G., Swaminathan, S., Beck, P., Steinhoff, M., Andrade-Gordon, P., Bunnett, N.W., Hollenberg, M.D., Wallace, J.L., Cirino, G., Fiorucci, S., 2004. A role for proteinase-activated receptor-1 in inflammatory bowel diseases. J. Clin. Invest. 114, 1444–1456.
Wang, H., Ubl, J.J., Stricker, R., Reiser, G., 2002. Thrombin (PAR-1)-induced proliferation in astrocytes via MAPK involves multiple signaling pathways. Am. J. Physiol. Cell Physiol. 283, C1351–C1364.
Wang, X.J., Kong, K.M., Qi, W.L., Ye, W.L., Song, P.S., 2005. Interleukin-1 beta induction of neuron apoptosis depends on p38 mitogen-activated protein kinase activity after spinal cord injury. Acta Pharmacol. Sin. 26, 934–942.
Wang, Y., Luo, W., Reiser, G., 2007. Proteinase-activated receptor-1 and −2 induce the release of chemokine GRO/CINC-1 from rat astrocytes via differential activation of JNK isoforms, evoking multiple protective pathways in brain. Biochem. J. 401, 65–78.
Wanner, I.B., Anderson, M.A., Song, B., Levine, J., Fernandez, A., Gray-Thompson, Z., Ao, Y., Sofroniew, M.V., 2013. Glial scar borders are formed by newly proliferated, elongated astrocytes that interact to corral inflammatory and fibrotic cells via STAT3-dependent mechanisms after spinal cord injury. J. Neurosci. 33, 12870–12886.
Wilhelmsson, U., Li, L., Pekna, M., Berthold, C.H., Blom, S., Eliasson, C., Renner, O., Bushong, E., Ellisman, M., Morgan, T.E., Pekny, M., 2004. Absence of glial fibrillary acidic protein and vimentin prevents hypertrophy of astrocytic processes and improves post-traumatic regeneration. J. Neurosci. 24, 5016–5021.
Yang, P., Wen, H., Ou, S., Cui, J., Fan, D., 2012. IL-6 promotes regeneration and functional recovery after cortical spinal tract injury by reactivating intrinsic growth program of neurons and enhancing synapse formation. Exp. Neurol. 236, 19–27.
Yoon, H., Radulovic, M., Wu, J., Blaber, S.I., Blaber, M., Fehlings, M.G., Scarisbrick, I.A., 2013. Kallikrein 6 signals through PAR1 and PAR2 to promote neuron injury and exacerbate glutamate neurotoxicity. J. Neurochem. 127, 283–298.
Yu, W.R., Fehlings, M.G., 2011. Fas/FasL-mediated apoptosis and inflammation are key features of acute human spinal cord injury: implications for translational, clinical application. Acta Neuropathol. 122, 747–761.